INTERNATIONAL ATOMIC ENERGY AGENCY
UNITED NATIONS EDUCATIONAL, SCIENTIFIC AND CULTURAL ORGANIZATION
INTERNATIONAL CENTRE FOR THEORETICAL PHYSICS
I.C.T.P., P.O. BOX 586, 34100 TRIESTE, ITALY, CABLE: CENTRATOM TRIESTE

H4.SMR/453-43

# TRAINING COLLEGE ON PHYSICS AND CHARACTERIZATION OF LASERS AND OPTICAL FIBRES

**(5 February - 2 March 1990)**

## FIBER TECHNOLOGIES

**A. Zuccala**

**F.O.S.**
**Battipaglia, Salerno**

FIBER TECHNOLOGIES

Teacher : Dr. Adriano Zuccala - FOS/PIRELLI

INDEX

# MATERIALS AND PROCESS FOR THE PRODUCTION OF OPTICAL FIBERS

( Adriano ZUCCALA )

Optical fibers are having a large diffusion in telecommunication field : potentiality of this trasmissive medium are exploited in terms of low attenuation and high bandwidth.
The attenuation level control is based upon the use of materials at very high purity,while the bandwidth depends on the refraction index profile of the fiber core.
The fiber is a glass line, with the standard external diameter of 125 $\mu$m ( except some fibers for special applications that can present different dimensions, i.e. 140 um ), coated with a polimeric material often applied in a double layer of different composition.
The glass presents, accross a section, a central area of appropriate dimensions and material composition, that is called " core " of the fiber, with a refractive index higher than the rest of the section, called " cladding ".
Due to the total reflection phenomenon, the light radiation injected into the core is guided by the transparent material without possibility of going into the cladding.
The main material used in optical fiber manufacturing is vitreous silica ( SiO2 ) : it presents the transparence and the chemical stability requested for this application.
The core is made doping the silica with others vitreous oxides, that have the capability of increase the refractive index.
The most largely used is GeO2, but also P2O 5 can be used.
B2O3 and F are suitable to eventually decrease the silica refractive index, and, for this reason they are mainly used to dope the cladding.
The very high purity of material used and the requested precision of the refractive index profile have lead to the set up of peculiar tecnics for fibers manufacturing.

First of all, it is not possible, even with the most sophisticated purification processes, to obtain a natural silica with the so low impurities level admitted ( few parts per billions ).
This fact has forced the use of a chemical synthesis process that allows, directly by reagents in vapour phase, to obtain synthetic silica, already doped with the others oxides in the quantity and form requested.
On the other end necessity of shaping with extreme precision the core index profile, enforces, for all the processes, the manufacturing of a semi - product ( preform or " blank " ) that as a glass cylinder already internally containing the chemical and, therefore, optical structure of the fiber, must be drawn in a further step.
Several processes, some of which have reached the industrial application phase, have been directly developed on the base of the common principle of the vapour phase deposition (CVD= = Chemical Vapour Deposition).
They are essentially divided in two large families : inside type process and ouside type process.
Each one of the two technics has been developed in different ways , that are able to produce optical waveguides of multimode type ( tipical core 50 $\mu$m ) and of singlemode type ( typical core 10 $\mu$m ).
Materials, half products and finished products themselves must undergo to rigorous control and qualification tests.
Geometrical and mechanical properties of the fiber must be also evaluated together with the optical characteristics.
Typical performances of the modern multimode fibers are : attenuation of 0.6 - 0.8 dB/Km at 1300 nm of wavelenght and corresponding bandwidth superior than 1 GHz . Km.
For monomode fibers attenuation of 0.35 dB/Km at 1300 nm and 0.22 - 0.25 dB/Km at 1550 nm are normal values.

# 4

# Optical Fibers, Cables and Connections

## 4.1 INTRODUCTION

Optical fiber waveguides and their transmission characteristics have been considered in some detail in Chapters 2 and 3. However, we have yet to discuss the practical considerations and problems associated with the production, application and installation of optical fibers within a line transmission system. These factors are of paramount importance if optical fiber communication systems are to be considered as viable replacements for conventional metallic line communication systems. Optical fiber communication is of little use if the many advantages of optical fiber transmission lines outlined in the previous chapters may not be applied in practice in the telecommunications network without severe degradation of their performance.

It is therefore essential that:

(a) Optical fibers may be produced with good stable transmission characteristics in long lengths at a minimum cost and with maximum reproducibility.
(b) A range of optical fiber types with regard to size, refractive indices and index profiles, operating wavelengths, materials, etc., be available in order to fulfill many different system applications.
(c) The fibers may be converted into practical cables which can be handled in a similar manner to conventional electrical transmission cables without problems associated with the degradation of their characteristics or damage.
(d) The fibers and fiber cables may be terminated and connected together (jointed) without excessive practical difficulties and in ways which limit the effect of this process on the fiber transmission characteristics to keep them within acceptable operating levels. It is important that these jointing techniques may be applied with ease in the field locations where cable connection takes place.

In this chapter we therefore pull together the various practical elements associated with optical fiber communications. Hence the various methods for preparing optical fibers (both liquid and vapor phase) with characteristics suitable for telecommunications applications are outlined in Sections 4.2 to 4.4.





This is followed in Section 4.5 with consideration of commercially available fibers describing in general terms both the types and their characteristics. The requirements for optical fiber cabling in relation to fiber protection are then discussed in Section 4.6 prior to consideration of cable design in Section 4.7. In Section 4.8 we deal with the losses incurred when optical fibers are connected together. This discussion provides a basis for consideration of the techniques employed for jointing optical fibers. Permanent fiber joints (or splices) are then dealt with in Section 4.9 prior to discussion of the various types of demountable fiber connector in Sections 4.10 to 4.12.

## 4.2 PREPARATION OF OPTICAL FIBERS

From the considerations of optical waveguiding of Chapter 2 it is clear that a variation of refractive index inside the optical fiber (i.e. between the core and the cladding) is a fundamental necessity in the fabrication of fibers for light transmission. Hence at least two different materials which are transparent to light over the operating wavelength range (0.8–1.6 μm) are required. In practice these materials must exhibit relatively low optical attenuation and they must therefore have low intrinsic absorption and scattering losses. A number of organic and inorganic insulating substances meet these conditions in the visible and near infrared regions of the spectrum.

However, in order to avoid scattering losses in excess of the fundamental intrinsic losses, scattering centers such as bubbles, strains and grain boundaries must be eradicated. This tends to limit the choice of suitable materials for the fabrication of optical fibers to either glasses (or glass like materials) and monocrystalline structures (certain plastics).

It is also useful, and in the case of graded index fibers essential, that the refractive index of the material may be varied by suitable doping with another compatible material. Hence these two materials should have mutual solubility over a relatively wide range of concentrations. This is only achieved in glasses or glass-like materials, and therefore monocrystalline materials are unsuitable for the fabrication of graded index fibers, but may be used for step index fibers. However, it is apparent that glasses exhibit the best overall material characteristics for use in the fabrication of low loss optical fibers. They are therefore used almost exclusively in the preparation of fibers for telecommunications applications. Plastic clad [Ref. 1] and all plastic fibers find some use in short haul, low bandwidth applications.

In this section the discussion will therefore be confined to the preparation of glass fibers. This is a two stage process in which initially the pure glass is produced and converted into a form (rod or preform) suitable for making the fiber. A drawing or pulling technique is then employed to acquire the end product. The methods of preparing the extremely pure optical glasses generally fall into two major categories which are:

(a) conventional glass refining techniques in which the glass is processed in the molten state (melting methods) producing a multicomponent glass structure;
(b) vapor phase deposition methods producing silica rich glasses which have melting temperatures that are too high to allow the conventional melt process.

These processes, with their respective drawing techniques, are described in the following sections.

## 4.3 LIQUID PHASE (MELTING) TECHNIQUES

The first stage in this process is the preparation of ultra pure material powders which are usually oxides or carbonates of the required constituents. These include oxides such as $SiO_2$, $GeO_2$, $B_2O_3$ and $Al_2O_3$, and carbonates such as

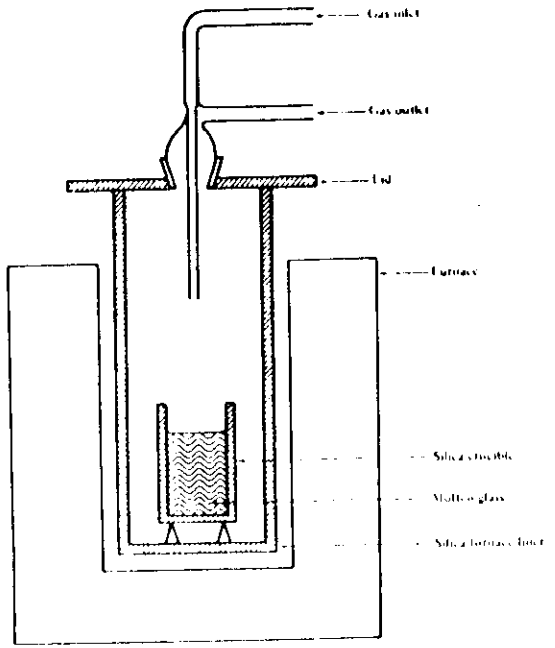

**Fig. 4.1** Glassmaking furnace for the production of high purity glasses [Ref. 4].



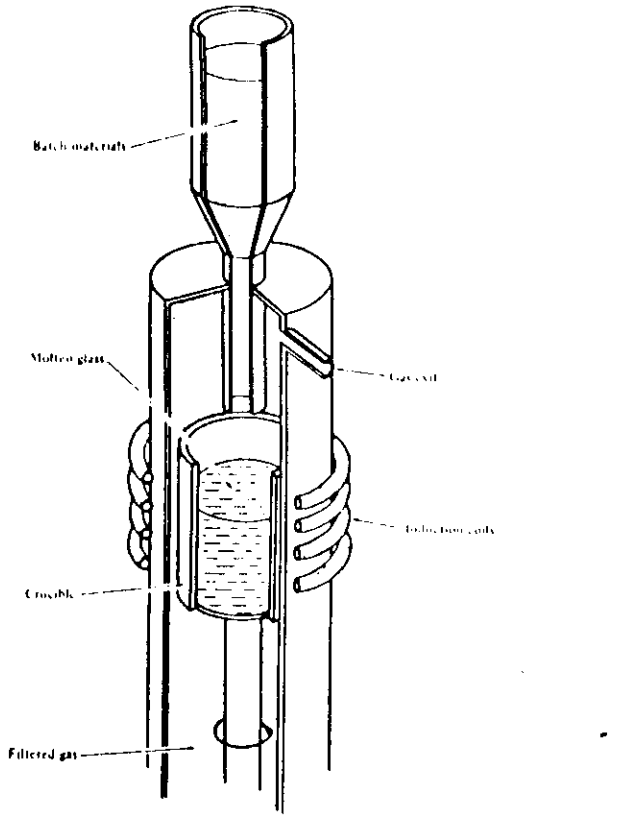


**Fig. 4.2** High purity glass melting using a radiofrequency induction furnace [Refs. 6-8].

$Na_2CO_3$, $K_2CO_3$, $CaCO_3$ and $BaCO_3$ which will decompose into oxides during the glass melting. Very high initial purity is essential and purification accounts for a large proportion of the material cost; nevertheless these compounds are commercially available with total transition metal contents below 20 parts in $10^9$ and below 1 part in $10^9$ for some specific impurities [Ref. 2]. The purification may therefore involve combined techniques of fine filtration and coprecipitation, followed by solvent extraction before recrystallization and final drying in a vacuum to remove any residual OH ions [Ref. 3].

The next stage is to melt these high purity, powdered, low melting point glass materials to form a homogeneous, bubble free multicomponent glass. A refractive index variation may be achieved by either a change in the composition of the various constituents or by ion exchange when the materials are in

the molten phase. The melting of these multicomponent glass systems occurs at relatively low temperatures between 900 and 1300 °C and may take place in a silica crucible as shown in Fig. 4.1 [Ref. 4]. However, contamination can arise during melting from several sources including the furnace environment and the crucible. Both fused silica and platinum crucibles have been used with some success although an increase in impurity content was observed when the melt was held in a platinum crucible at high temperatures over long periods [Ref. 5].

Silica crucibles can give dissolution into the melt which may introduce inhomogeneities into the glass especially at high melting temperatures. A technique for avoiding this involves melting the glass directly into a radio-frequency (RF approximately 5 MHz) induction furnace while cooling the silica by gas or water flow as shown in Fig. 4.2 [Refs. 6–8]. The materials are preheated to around 1000 °C where they exhibit sufficient ionic conductivity to enable coupling between the melt and the RF field. The melt is also protected from any impurities in the crucible by a thin layer of solidified pure glass which forms due to the temperature difference between the melt and the cooled silica crucible.

In both techniques the glass is homogenized and dried by bubbling pure gases through the melt, whilst protecting against any airborne dust particles either originating in the melt furnace or present as atmospheric contamination. After the melt has been suitably processed, it is cooled and formed into long rods (cane) of multicomponent glass.

### 4.3.1 Fiber Drawing

The traditional technique for producing fine optical fiber waveguides is to make a preform using the rod in tube process. A rod of core glass is inserted into a tube of cladding glass and the preform is drawn in a vertical muffle furnace as illustrated in Fig. 4.3 [Ref. 9]. This technique is useful for the production of step index fibers with large core and cladding diameters where the achievement of low attenuation is not critical as there is a danger of including bubbles and particulate matter at the core–cladding interface.

Another technique which is also suitable for the production of large core diameter step index fibers, and reduces the core–cladding interface problems, is called the stratified melt process. This process, developed by Pilkington Laboratories [Ref. 10], involves pouring a layer of cladding glass over the core glass in a platinum crucible as shown in Fig. 4.4 [Ref. 11]. A bait glass rod is dipped into the molten combination and slowly withdrawn giving a composite core-clad preform which may be then drawn into a fiber.

Subsequent development in the drawing of optical fibers (especially graded index) produced by liquid phase techniques has concentrated on the double crucible method. In this method the core and cladding glass in the form of separate rods is fed into two concentric platinum crucibles as illustrated in



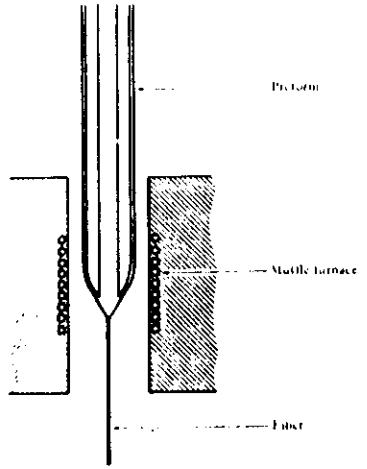

Fig. 4.3 Optical fiber from a preform [Ref. 9].

Fig. 4.5 [Ref. 4]. The assembly is usually located in a muffle furnace capable of heating the crucible contents to a temperature of between 800 and 1200 °C. The crucibles have nozzles in their bases from which the clad fiber is drawn directly from the melt as shown in Fig. 4.5. Index grading may be achieved through the diffusion of mobile ions across the core–cladding interface within the molten glass. It is possible to achieve a reasonable refractive index profile via this diffusion process, although due to lack of precise control it is not possible to obtain the optimum near parabolic profile which yields the

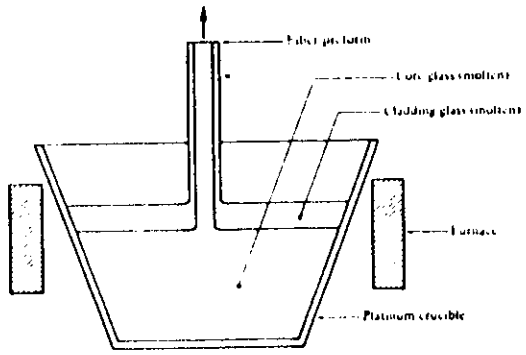

Fig. 4.4 The stratified melt process (glass on glass technique) for producing glass clad rods or preforms [Ref. 11].

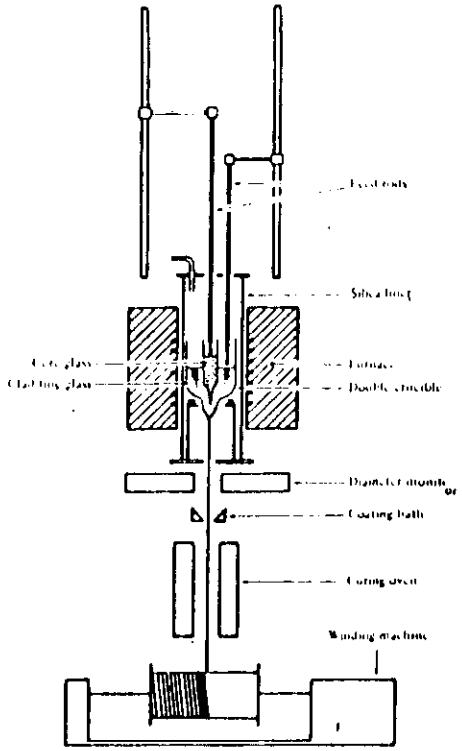

Fig. 4.5 The double crucible method for fiber drawing [Ref. 4]

minimum pulse dispersion (see Section 3.9.2). Hence graded index fibers produced by this technique are substantially less dispersive than step index fibers, but do not have the bandwidth–length products of optimum profile fibers. Pulse dispersion of 1–6 ns km$^{-1}$ [Refs. 12, 13] is quite typical, depending on the material system used.

Some of the material systems used in the fabrication of multicomponent glass step index and graded index fibers are given in Table 4.1.

Using very high purity melting techniques and the double crucible drawing method, step index and graded index fibers with attenuations as low as 3.4 dB km$^{-1}$ [Ref. 14] and 1.1 dB km$^{-1}$ [Ref. 2] respectively have been produced. However, such low losses cannot be consistently obtained using liquid phase techniques and typical losses for multicomponent glass fibers prepared continuously by these methods are between 5 and 10 dB km$^{-1}$. Therefore, liquid phase techniques have the inherent disadvantage of obtaining



Table 4.1 Material systems used in the fabrication of multicomponent glass fibers by the double crucible technique

| **Step Index** | |
|---|---|
| Core glass | Cladding glass |
| $Na_2O$-$B_2O_3$-$SiO_2$ | $Na_2O$-$B_2O_3$-$SiO_2$ |
| $Na_2O$-$Li_2O$-$CaO$-$SiO_2$ | $Na_2O$-$Li_2O$-$CaO$-$SiO_2$ |
| $Na_2O$-$CaO$-$GeO_2$ | $Na_2O$-$CaO$-$SiO_2$ |
| $Tl_2O$-$Na_2O$-$B_2O_3$-$GeO_2$-$BaO$-$CaO$-$SiO_2$ | $Na_2O$-$B_2O_3$-$SiO_2$ |
| $Na_2O$-$BaO$-$GeO_2$-$B_2O_3$-$SiO_2$ | $Na_2O$-$B_2O_3$-$SiO_2$ |
| $P_2O_5$-$Ga_2O_3$-$GeO_2$ | $P_2O_5$-$Ga_2O_3$-$SiO_2$ |
| **Graded Index** | |
| Base glass | Diffusion mechanism |
| $R_2O$-$GeO_2$-$CaO$-$SiO_2$ | $Na^+ = K^+$ |
| $R_2O$-$B_2O_3$-$SiO_2$ | $Tl^+ = Na^+$ |
| $Na_2O$-$B_2O_3$-$SiO_2$ | $Na_2O$ diffusion |
| $Na_2O$-$B_2O_3$-$SiO_2$ | $CaO$, $BaO$ diffusion |

and maintaining extremely pure glass which limits their ability to produce low loss fibers. The advantage of these techniques is in the possibility of continuous production (both melting and drawing) of optical fibers.

## 4.4 VAPOR PHASE DEPOSITION TECHNIQUES

Vapor phase deposition techniques are used to produce silica rich glasses of the highest transparency and with the optimal optical properties. The starting materials are volatile compounds such as $SiCl_4$, $GeCl_4$, $SiF_4$, $BCl_3$, $O_2$, $BBr_3$ and $POCl_3$ which may be distilled to reduce the concentration of most transition metal impurities to below one part in $10^9$ giving negligible absorption losses from these elements. Refractive index modification is achieved through the formation of dopants from the nonsilica starting materials. These vapor phase dopants include $TiO_2$, $GeO_2$, $P_2O_5$, $Al_2O_3$, $B_2O_3$ and F, the effects of which on the refractive index of silica are shown in Fig. 4.6 [Ref. 2]. Gaseous mixtures of the silica containing compound, the doping material and oxygen are combined in a vapor phase oxidation reaction where the deposition of oxides occurs. The deposition is usually onto a substrate or within a hollow tube and is built up as a stack of successive layers. Hence the dopant concentration may be varied gradually to produce a graded index profile or maintained to give a step index profile. In the case of the substrate this directly results in a solid rod or preform whereas the hollow tube must be collapsed to give a solid preform from which the fiber may be drawn.

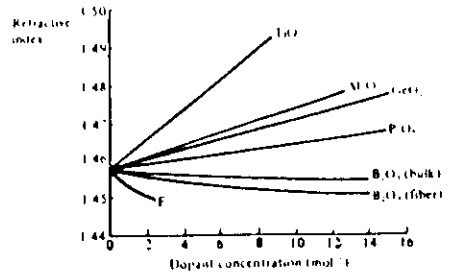

**Fig. 4.6** The variation in the refractive index of silica using various dopants. Reproduced with permission from the publishers, Society of Glass Technology. *Phys Chem Glasses*, **21** p 5, 1980.

There are a number of variations of vapor phase deposition which have been successfully utilized to produce low loss fibers. The major techniques are illustrated in Fig. 4.7, which also indicates the plane (horizontal or vertical) in which the deposition takes place as well as the formation of the preform. These vapor phase deposition techniques fall into two broad categories: flame hydrolysis and chemical vapor deposition (CVD) methods. The individual techniques are considered in the following sections.

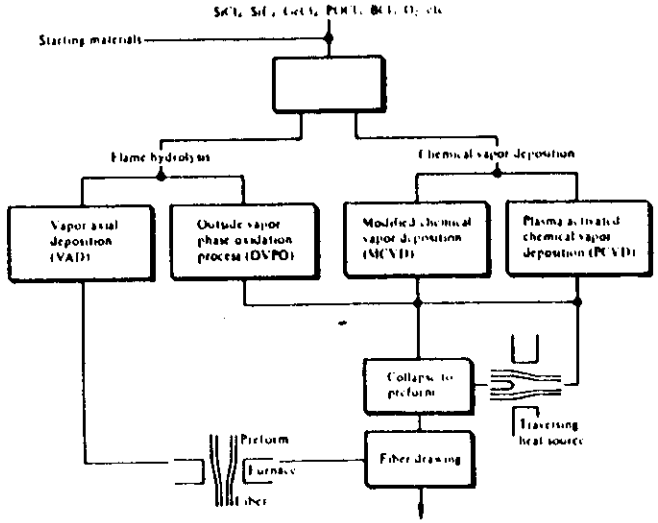


**Fig. 4.7** Schematic illustration of the vapor phase deposition techniques used in the preparation of low loss optical fibers.



### 4.4.1 Outside Vapor Phase Oxidation (OVPO) Process

This process which uses flame hydrolysis stems from work on 'soot' processes originally developed by Hyde [Ref. 17] which were used to produce the first fiber with losses of less than 20 dB km$^{-1}$ [Ref. 18]. The best known technique of this type is often referred to as the outside vapor phase oxidation process. In this process the required glass composition is deposited laterally from a 'soot' generated by hydrolyzing the halide vapors in an oxygen–hydrogen flame. Oxygen is passed through the appropriate silicon compound (i.e. $SiCl_4$) which is vaporized, removing any impurities. Dopants such as $GeCl_4$ or $TiCl_4$ are added and the mixture is blown through the oxygen–hydrogen flame giving the following reactions:

$$\underset{\text{(vapor)}}{SiCl_4} + \underset{\text{(vapor)}}{2H_2O} \xrightarrow{\text{heat}} \underset{\text{(solid)}}{SiO_2} + \underset{\text{(gas)}}{4HCl} \qquad (4.1)$$

and

$$\underset{\text{(vapor)}}{SiCl_4} + \underset{\text{(gas)}}{O_2} \xrightarrow{\text{heat}} \underset{\text{(solid)}}{SiO_2} + \underset{\text{(gas)}}{2Cl_2} \qquad (4.2)$$

$$\underset{\text{(vapor)}}{GeCl_4} + \underset{\text{(gas)}}{O_2} \xrightarrow{\text{heat}} \underset{\text{(solid)}}{GeO_2} + \underset{\text{(gas)}}{2Cl_2} \qquad (4.3)$$

or

$$\underset{\text{(vapor)}}{TiCl_4} + \underset{\text{(gas)}}{O_2} \xrightarrow{\text{heat}} \underset{\text{(solid)}}{TiO_2} + \underset{\text{(gas)}}{2Cl_2} \qquad (4.4)$$

The silica is generated as a fine soot which is deposited on a cool rotating mandrel as illustrated in Fig. 4.8(a) [Ref. 19]. The flame of the burner is traversed back and forth over the length of the mandrel until a sufficient number of layers of silica (approximately 200) are deposited on it. When this process is completed the mandrel is removed and the porous mass of silica soot is sintered (to form a glass body) as illustrated in Fig. 4.8(b). The preform may contain both core and cladding glasses by properly varying the dopant concentrations during the deposition process. Several kilometers (around 10 km of 120 μm core diameter fiber have been produced [Ref. 2]) can be drawn from the preform by collapsing and closing the central hole as shown in Fig. 4.8(c). Fine control of the index gradient for graded index fibers may be achieved using this process as the gas flows can be adjusted at the completion of each traverse of the burner. Hence fibers with bandwidth–length products as high as 3 GHz km have been achieved [Ref. 20] through accurate index grading with this process.

The purity of the glass fiber depends on the purity of the feeding materials

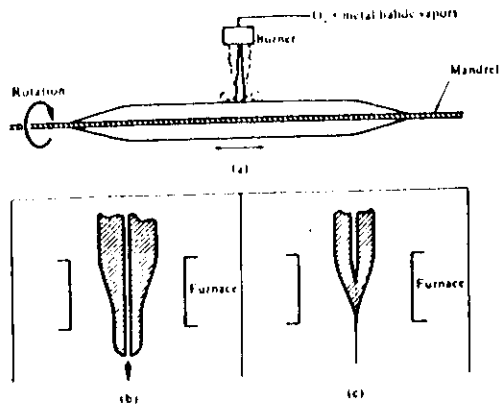


**Fig. 4.8** Schematic diagram of the OVPO process for the preparation of optical fibers: (a) soot deposition, (b) preform sintering, (c) fiber drawing [Ref. 19].

and also upon the amount of OH impurity from the exposure of the silica to water vapor in the flame following the reactions given in Eqs. (4.1) to (4.4). Typically the OH content is between 50 and 200 parts per million and this contributes to the fiber attenuation. It is possible to reduce the OH impurity content by employing gaseous chlorine as a drying agent during sintering. This has given losses as low as 1 dB $km^{-1}$ and 1.8 dB $km^{-1}$ at wavelengths of 1.2 and 1.55 μm respectively [Ref. 21] in fibers prepared using the OVPO process.

Other problems stem from the use of the mandrel which can create some difficulties in the formation of the fiber preform. Cracks may form due to stress concentration on the surface of the inside wall when the mandrel is removed. Also the refractive index profile has a central depression due to the collapsed hole when the fiber is drawn. Therefore although the OVPO process is a useful fiber preparation technique, it has several drawbacks. Furthermore it is a batch process which limits its use for the volume production of optical fibers.

### 4.4.2 Vapor Axial Deposition (VAD)

This process was developed by Izawa *et al.* [Ref. 22] in the search for a continuous (rather than batch) technique for the production of low loss optical fibers. The VAD technique uses an end-on deposition onto a rotating fused silica target as illustrated in Fig. 4.9 [Ref. 23]. The vaporized constituents are injected from burners and react to form silica soot by flame hydrolysis. This is deposited on the end of the starting target in the axial direction forming a solid porous glass preform in the shape of a boule. The preform which is growing in the axial direction is pulled upwards at a rate which corresponds to the growth



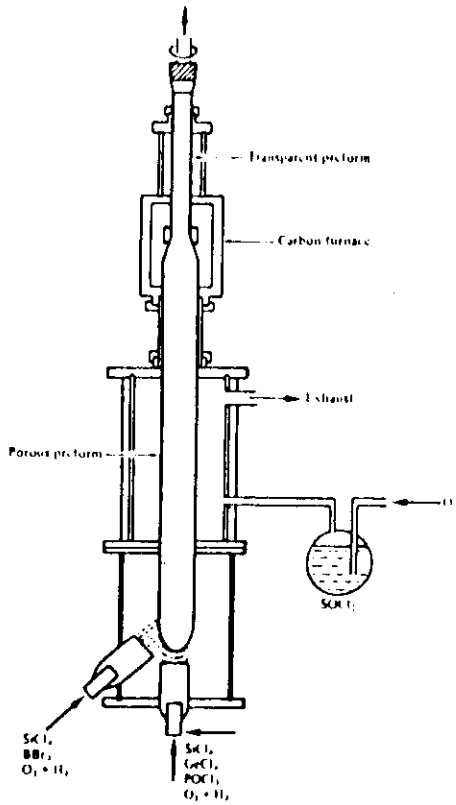


**Fig. 4.9** The VAD process [Ref. 23].

rate. It is initially dehydrated by heating with $SOCl_2$ using the reaction:

$$\underset{\text{(vapor)}}{H_2O} + \underset{\text{(vapor)}}{SOCl_2} \xrightarrow{\text{heat}} \underset{\text{(gas)}}{2HCl} + \underset{\text{(gas)}}{SO_2} \qquad (4.5)$$

and is then sintered into a solid preform in a graphite resistance furnace at an elevated temperature of around 1500 °C. Therefore, in principle this process may be adapted to draw fiber continuously, although at present it tends to be operated as a batch process.

A spatial refractive index profile may be achieved using the deposition properties of $SiO_2$–$GeO_2$ particles within the oxygen–hydrogen flame. The concentration of these constituents deposited on the porous preform is controlled by the substrate temperature distribution which can be altered by

changing the gas flow conditions. Fibers produced by the VAD process still suffer from some OH impurity content due to the flame hydrolysis and hence very low loss fibers have not been achieved using this method. Nevertheless, fibers with attenuation in the range 0.7–2.0 dB km$^{-1}$ at a wavelength of 1.18 μm have been reported [Ref. 24].

### 4.4.3 Modified Chemical Vapor Deposition (MCVD)

Chemical vapor deposition techniques are commonly used at very low deposition rates in the semiconductor industry to produce protective $SiO_2$ films on silicon semiconductor devices. Usually an easily oxidized reagent such as $SiH_4$ diluted by inert gases and mixed with oxygen is brought into contact with a heated silicon surface where it forms a glassy transparent silica film. This heterogeneous reaction (i.e. requires a surface to take place) was pioneered for the fabrication of optical fibers using the inside surface of a fused quartz tube [Ref. 25]. However, these processes gave low deposition rates and were prone to OH contamination due to the use of hydride reactants. This led to the development of the modified chemical vapor deposition (MCVD) process by Bell Telephone Laboratories [Ref. 26] and Southampton University, UK [Ref. 27], which overcomes these problems and has found widespread application throughout the world.

The MCVD process is also an inside vapor phase oxidation (IVPO) technique taking place inside a silica tube as shown in Fig. 4.10. However, the vapor phase reactants (halide and oxygen) pass through a hot zone so that a substantial part of the reaction is homogeneous (i.e. involves only one phase; in

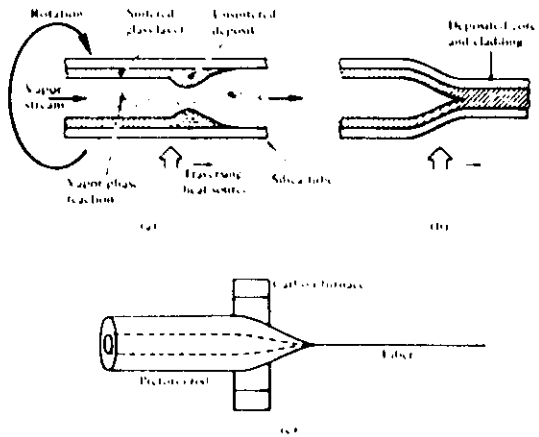

**Fig. 4.10** Schematic diagram showing the MCVD method for the preparation of optical fibers. (a) deposition, (b) collapse to produce a preform, (c) fiber drawing



this case the vapor phase). Glass particles formed during this reaction travel with the gas flow and are deposited on the walls of the silica tube. The tube may form the cladding material but usually it is merely a supporting structure which is heated on the outside by an oxygen–hydrogen flame to temperatures between 1400 °C and 1600 °C. Thus a hot zone is created which encourages high temperature oxidation reactions such as those given in Eqs. (4.2) and (4.3) or (4.4) (not Eq. (4.1)). These reactions reduce the OH impurity concentration to levels below those found in fibers prepared by hydride oxidation or flame hydrolysis.

The hot zone is moved back and forth along the tube allowing the particles to be deposited on a layer by layer basis giving a sintered transparent silica film on the walls of the tube. The film may be up to 10 μm in thickness and uniformity is maintained by rotating the tube. A graded refractive index profile can be created by changing the composition of the layers as the glass is deposited. Usually when sufficient thickness has been formed by successive traverses of the burner for the cladding, vaporized chlorides of germanium ($GeCl_4$) or phosphorus ($POCl_3$) are added to the gas flow. The core glass is then formed by the deposition of successive layers of germanosilicate or phosphosilicate glass. The cladding layer is important as it acts as a barrier which suppresses OH absorption losses due to the diffusion of OH ions from the silica tube into the core glass as it is deposited. After the deposition is completed the temperature is increased to between 1700 and 1900 °C. The tube is then collapsed to give a solid preform which may then be drawn into fiber at temperatures of 2000–2200 °C as illustrated in Fig. 4.10.

This technique is the most widely used at present as it allows the fabrication of fiber with the lowest losses. Apart from the reduced OH impurity contamination the MCVD process has the advantage that deposition occurs within an enclosed reactor which ensures a very clean environment. Hence gaseous and particulate impurities may be avoided during both the layer deposition and the preform collapse phases. The process also allows the use of a variety of materials and glass compositions. It has produced $GeO_2$ doped silica single mode fiber with minimum losses of only 0.2 dB km$^{-1}$ at a wavelength of 1.55 μm [Ref. 28]. More generally the $GeO_2$–$B_2O_3$–$SiO_2$ system ($B_2O_3$ is added to reduce the viscosity and assist fining) has shown minimum losses of 0.34 dB km$^{-1}$ with multimode fiber at a wavelength of 1.55 μm [Ref. 29]. Also graded index germanium phosphosilicate fibers have exhibited losses near the intrinsic level for their composition of 2.8, 0.45 and 0.35 dB km$^{-1}$ at wavelengths of 0.82, 1.3 and 1.5 μm respectively [Ref. 30].

The MCVD process has also demonstrated the capability of producing fibers with very high bandwidths, although still well below the theoretical values which may be achieved. Multimode graded index fibers with measured bandwidth–length products of 4.3 GHz km and 4.7 GHz km at wavelengths of 1.25 and 1.29 μm have been reported [Ref. 31]. Large scale batch production

(30,000 km) of 50 μm core graded index fiber has maintained bandwidth–length products of 825 MHz km and 735 MHz km at wavelengths of 0.825 and 1.3 μm respectively [Ref. 30]. The median attenuation obtained with this fiber was 3.4 dB km$^{-1}$ at 0.825 μm and 1.20 dB km$^{-1}$ at 1.3 μm. Hence, although it is not a continuous process, the MCVD technique has proved suitable for the mass production of high performance optical fiber.

### 4.4.4 Plasma-activated Chemical Vapor Deposition (PCVD)

A variation on the MCVD technique is the use of various types of plasma to supply energy for the vapor phase oxidation of halides. This method, first developed by Kuppers and Koenings [Ref. 32], involves plasma induced chemical vapor deposition inside a silica tube as shown in Fig. 4.11. The essential difference between this technique and the MCVD process is the stimulation of oxide formation by means of a nonisothermal plasma maintained at low pressure in a microwave cavity (2.45 GHz) which surrounds the tube. Volatile reactants are introduced into the tube where they react heterogeneously within the microwave cavity and no particulate matter is formed in the vapor phase.

The reaction zone is moved backwards and forwards along the tube by control of the microwave cavity and a circularly symmetric layer growth is formed. Rotation of the tube is unnecessary and the deposition is virtually 100% efficient. Film deposition can occur at temperatures as low as 500 °C, but a high chlorine content may cause expansivity and cracking of the film. Hence the tube is heated to around 1000 °C during deposition using a stationary furnace.

The high deposition efficiency allows the composition of the layers to be accurately varied by control of the vapor phase reactants. Also when the plasma zone is moved rapidly backwards and forwards along the tube very thin layer deposition may be achieved giving the formation of up to 2000 individual layers. This enables very good graded index profiles to be realized which are a close approximation to the optimum near parabolic profile. Thus low pulse dispersion of less than 0.8 ns km$^{-1}$, for fibers with attenuations of between 3 and 4 dB km$^{-1}$, at a wavelength of 0.85 μm have been reported [Ref. 2].

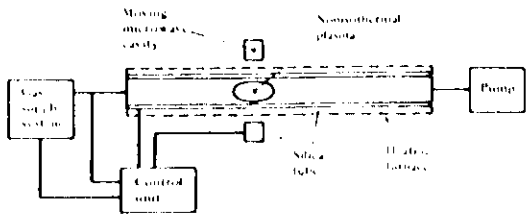


**Fig. 4.11** The apparatus utilized in the PCVD process



A further PCVD technique uses an inductively coupled radiofrequency argon plasma which operates at a frequency of 3.4 MHz [Ref. 33]. The deposition takes place at 1 atmosphere pressure and is predominantly a homogeneous vapor phase reaction which, via the high temperature discharge, causes the fusion of the deposited material into glass. This technique has proved to have a reaction rate five times faster than the conventional MCVD process. However, fiber attenuation is somewhat higher with losses of 6 dB km$^{-1}$ at a wavelength of 1.06 μm. Variations on this theme operating at frequencies of 3–6 MHz and 27 MHz have produced $GeO_2$–$P_2O_5$–$SiO_2$ fibers with minimum losses of 4–5 dB km$^{-1}$ at a wavelength of 0.85 μm [Ref. 34].

# OPTICAL FIBER MANUFACTURING IN FOS

( A. Zuccala )

## 1) INTRODUCTION

FOS optical fibers are manufactured with the Outside Vapor Deposition (OVD) process.

The OVD process is made up of three process steps:

. The first step is soot deposition. A hot stream of soot particles of desired composition is generated by passing the vapor stream through a fuel gas-oxigen flame directed towards a rotating and traversing refractory target rod. The soot particles are deposited on this rod in a partially sintered state and, layer by layer, a cylindrical porous glass preform is built up.
When enough glass is deposited for both the core and the cladding of the optical fiber, deposition is stopped and the porous preform is slipped off the target rod.

. The porous preform is then taken to the second process step of sintering. In this process step the preform is zone sintered, at temperatures between 1400°- 1600°C depending on glass composition, to a solid, bubble-free, glass blank by passing it through a furnace hot zone in a controlled atmosphere. At this stage the central hole due to removal of the target rod may or may not remain.

. The glass blank with or without the central hole can then be drawn into a fiber at much higher temperature of 2100 - 2200 C.

## 2) PROCESS DESCRIPTION

. The chemical reactions involved in the formation of the glass soot are complex, involving not only the SiCl4, GeCl4 and O2, but also the fuel gas (CH4 or H2) combustion products.
The chlorides react with O2, Equations (1) and (2), as they are heated to above 1500°C in the flame.

1) $SiCl_4 + O_2 \rightarrow SiO_2 + 2\ Cl_2$

2) $GeCl_4 + O_2 \rightleftharpoons GeO_2 + 2\ Cl_2$.

Equations (2) is shown as being in equilibrium because GeO2 is not significantly more stable than GeCl4 at these temperatures.
The glass particle formation (SiO2) has been shown to begin within about 10 mm from the burner face and is nearly complete within 100 mm. Typically the particles formed are on the order of 0.1 µm ÷ 0.25 µm and they vary in size throughout the flame.
Due to the small size of the particles, they cannot be collected by impaction because they tend to follow the gas streamlines. Careful analysis of the collection of soot particles onto a porous preform indicates that

thermophoresis is the dominant mechanism for collection. In studies to maximize deposition rate from a single OVD burner it has been demonstrated that, for a given burner, two key parameters are: target diameter (of the preform) and fuel glass flow. The average collection efficiency of the OVD is around 50%.

. The most significant feature of the process step of drying and sintering consists in the way drying gases are fed into the preform within the furnace environment. In the OVD process, the removal of the target rod makes it possible to deliver the drying gases through this centerhole as the preform is fed down through the sintering furnace. Although the elimination of all hidroxyl ions from the preform is attempted, the radial hydroxyl ion gradient, if any, is favourable for propagation of light in the core of the fiber when this approach is used. This is considered to be an important feature of the OVD process that has made possible to obtain a very high level of drying in OVD fibers.

. The next step is fiber drawing. This is done by placing a sintered preform into a high temperature furnace, where the tip of the preform is heated to between 2100° ÷ 2200° C, and then it is free-drawn to a fiber with diameter of 125 $\mu$m.

A capstan pulling apparatus is used for free drawing of the fiber. During drawing, the core and cladding glasses maintain their respective geometric relationship, even though diameter reductions are as high as 300 : 1. Below the furnace is a laser gauge that monitors the fiber diameter followed by the applications of two layers of polymeric coating materials. The coatings are necessary to preserve the high intrinsic strenght, to provide microbending protection and to allow handling of the fiber. Subsequent to coating, the fiber passes through the capstan drive and the tensile strenght monitor before being wound on a drum. The fiber is then transferred for optical, geometrical, mechanical characterization. (see Final Measurement (FM) manual).

# Outside Vapor Deposition

A. J. Morrow  P. C. Schultz

TR 41/March 1984

## Introduction

This paper deals with the outside vapor deposition (OVD) process of manufacturing glass preforms for optical waveguide fibers. The OVD process is one of the three major processes used in the world today to manufacture optical waveguides. The other two processes are the Modified Chemical Vapor Deposition (MCVD) and Vapor Axial Deposition (VAD) processes. At the onset, it is important to note that in attempting to compile material for this paper, prior knowledge of the basic physics of all components of fiber-optic communication systems has been assumed.

The most widely used optical waveguide manufacturing process is the MCVD process. Compared to the MCVD process the OVD process is significantly more complex. This complexity and the need for custom designed equipment have caused restrictive use of this process around the world. Of all the major optical waveguide manufacturers only Corning Glass Works, the company where the process was invented, uses this process to manufacture optical fibers. Although complex, Corning believes it to be a very flexible and economic process capable of producing high quality fibers for diverse applications. The process has been successfully industrialized and automated. It is the primary process used to manufacture optical waveguides in Corning's manufacturing plant at Wilmington, N.C. The race towards economic manufacturing of high-quality fiber optics is just beginning and the market is in constant flux with new products. There is also an ongoing proliferation of new applications. A dominant process, if ever, is not likely to emerge in this decade, but the OVD process has the potential to fulfill all the requirements as they are presently understood.

This paper is organized in four sections. The rest of this introductory first section will cover the background of the OVD process and includes the process description. The second section will be devoted to the basic understanding of the process steps. The various products manufactured by the OVD process and their performance characteristics will be described in the third section. The fourth, and last, section will summarize the state of the art of the process and provide early results of some developmental activities in OVD.

Because of the complexity of the subject, an explanation of only the basic concepts of what makes OVD work and how is attempted. In doing this, vigorous mathematical analysis has had to be minimized.

## Background on Vapor Deposition Processes

In order to put the OVD process in proper perspective, it is important to differentiate between two basically different classes of chemical vapor deposition (CVD) processes. The most commonly known is that used primarily in the fabrication of semiconductor devices. Typically, a low pressure, low concentration vapor stream of organometallics or metal halides is reacted at or near a heated substrate surface resulting in, ideally, a uniform, defect-free deposition on the substrate. The reaction can be heterogeneous (occurring on the surface) or homogeneous (occurring in the vapor phase). Rates are low because the aim is to deposit essentially molecular layers of crystalline solid. Also, the surface available for deposition is limited in area.

The class of CVD most commonly used for fabrication of bulk glass products is quite different. It relies on thermally activated homogeneous (vapor phase) oxidation reactions of starting mixtures of metal halides and oxygen. Glassy particles called "soot" are nucleated and grow and are subsequently deposited on a substrate or target. They can be fused to form a clear glass object or collected as a porous preform—depending on temperature. This application typically uses much larger concentrations of reactants and is operated at ambient pressure. As a result, deposition rate



can be more than an order of magnitude greater than in the previously described case. The target, or substrate, can also be much larger in area allowing more efficient collection. Not surprisingly, the majority of fiber optics manufacturing techniques, including OVD, MCVD, and VAD are examples of this class of CVD process.

One of the first bulk glass products manufactured by such a vapor deposition process was fused silica by Corning Glass Works (Hyde, 1942). It was also the process concept Corning scientists used in their historical breakthrough of producing the first $\lesssim$ 20 dB/km glass fiber (Kapron, et al., 1970). This success led to extensive worldwide effort to develop vapor deposition processes to manufacture practical optical fibers and a rapidly growing optical communications industry. This effort in Corning Glass Works led to the development of the OVD process.

## OVD Process Description

The OVD process is made up of three process steps shown in Figure 1. The first step is soot deposition. In this step a hot stream of soot particles of desired composition is generated by passing the vapor stream through a fuel gas oxygen flame directed towards a rotating and traversing refractory target rod. The soot particles are deposited on this rod in a partially sintered state and, layer by layer, a cylindrical porous glass preform is built up. When enough glass is deposited for both the core and the cladding of the optical fiber, deposition is stopped and the porous preform is slipped off the target rod.

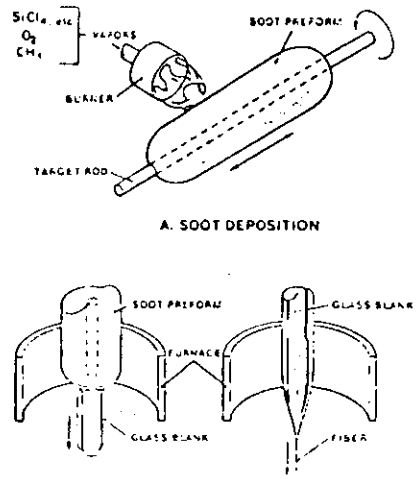


Outside Vapor Deposition (OVD) Process Steps.

Figure 1

The porous preform is then taken to the second process step of sintering. In this process step the preform is zone sintered, at temperatures between 1400-1600°C depending on glass composition, to a solid, bubble-free, glass blank by passing it through a furnace hot zone in a controlled atmosphere. At this stage the central hole due to removal of the target rod may or may not remain. The glass blank with or without the central hole can then be drawn into a fiber at much higher temperatures of 1800-2200°C.

## Evolution of OVD Technology

In the early to mid seventies, exploratory work on the process emphasized materials research. The initial concept of using dopants having the required purity level as high vapor pressure liquids or gases was considered to be very restrictive. Most such dopants, that were primarily used in the semiconductor industry, raised the Rayleigh scattering coefficient of fused silica. The search for low loss materials was focused on compositions that would have low intrinsic loss, i.e. low Rayleigh scattering loss and low loss due to IR and UV absorption band edges, in the operating wavelengths of interest. Theoretical analysis of such compositions led to efforts to produce these by vapor deposition techniques.

Two modifications to utilize raw materials available as low vapor pressure liquids (Randall, 1975a) or as solids (Randall, 1975b) are shown in Figures 2 and 3. In attempting to utilize low vapor pressure liquids, Figure 2, silicon tetrachloride is conventionally transported into an oxy-gas burner as a vapor stream. The liquid dopant raw material is pressurized and passed through a nebulizer into

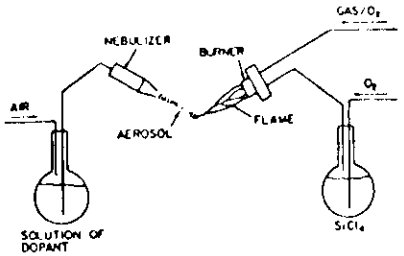


Dopant delivery using nebulizer for low vapor pressure liquids (Randall, 1975a).

Figure 2

the flame where thermal decomposition occurs producing the desired oxide. The soot is collected as a porous preform, homogeneous in composition of silica and dopant, layer by layer. All the downstream processing steps are the same as that produced from high vapor pressure liquids. The second concept, Figure 3, starts with solid dopants

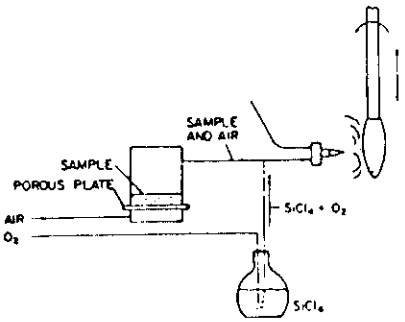


Dopant delivery using a porous plate injection device for liquids or solids (Randall, 1975b).

Figure 3

which are incorporated and transported along the vapor stream and fed into the burner. The materials may be sublimated or simply injected into the vapor stream as very small particles depending on vapor pressure.

A second approach to doping silica is in the consolidation process step. Extensive work has

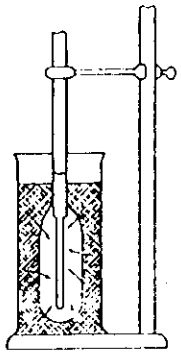

Doping by impregnation with liquid dopant solution (Schultz, 1975).

Figure 4

also been expended on this approach. Figure 4 (Schultz, 1975) shows a method of impregnating a porous OVD silica preform with a liquid phase dopant. Figure 5 (Dumbaugh and Schultz, 1975)

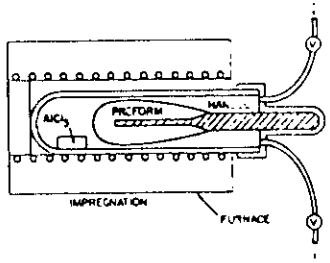


Doping by gaseous impregnation (Dumbaugh and Schultz, 1975).

Figure 5

shows gaseous impregnation with the starting material being a high purity, high vapor pressure solid such as $AlCl_3$.

These early studies of depositing glasses of various compositions were inspired by the belief that direct melting of solid raw materials could, on a routine basis, produce fibers of comparable optical loss to those produced by vapor deposition techniques.



The simplest of the possible approaches, that of using high vapor pressure liquid or gaseous starting materials, was found to be compatible with the OVD process. Merely by extending semiconductor raw materials into glass making, dopants such as germanium dioxide, phosphorous pentoxide, boron sesquioxide, and fluorine were identified. Not only did these dopants produce low loss fibers, but the losses came down so dramatically in a matter of four to five years that an entire new industry emerged. The success of this development pre-empted the process research on alternative approaches described above. However, despite the fact they were never shown feasible as useful approaches for making optical fibers, they could indeed be useful for making high purity glasses of various diverse compositions.

## OVD Process Steps

The OVD process may be broken down into its basic elements for comparison to the other processes of fabricating optical fibers by vapor deposition. This approach, although simplistic in nature, will help focus on the process steps unique to the OVD process and not fully covered elsewhere. The process can be broken down as follows:

A. Purification of raw materials.
B. Transport of reactants to heat source.
C. Chemical reactions and particle formation.
D. Particle collection.
E. Drying and sintering.
F. Preform design.

## Purification of Raw Materials

Purification in terms of inorganic ions is important to not only all the processes for producing optical fibers, but for the semiconductor technologies as well. The raw material manufacturers of silicon, germanium, phosphorous, boron, and fluorine compounds for use in vapor deposition processes have developed purification technology that is adequate for optical fiber manufacturing. An extension of the purification state-of-the art was required for the MCVD process, however, where hydroxyl ion content of the fiber is controlled at the deposition stage (Barns, *et al*., 1980).

This is not critical to the OVD process, since hydroxyl ion content is controlled in the consolidation process step.

## Transport of Reactants to Heat Source

The ability to transport an accurate composition of reactants to the heat source is critical not only to fiber tolerances but also to controlling performance characteristics of fibers. The most common vapor delivery system is called a "bubbler system" and is schematically shown in Figure 6. In this case a

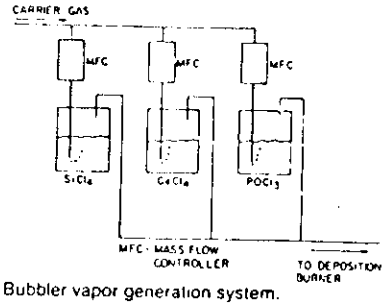


Bubbler vapor generation system.

Figure 6

carrier gas is bubbled through the high vapor pressure liquid reactant. A certain amount of reactant vapor is entrapped into the vapor stream. This is simply an evaporation process. Control of an evaporation process and its key parameters are well known and will not be described here. It is, however, important to point out some of the implementation schemes commonly used regarding the following parameters: 1) choice of carrier gas, 2) flow control, 3) temperature control, 4) saturation control and 5) material of construction. It is also important to point out that these choices are still differently made in different laboratories. Convergence in opinion and approach may come later as the technology matures.

1) The choice of carrier gas has been of two kinds. Oxygen, a key reactant, has been used as a carrier gas. This approach benefits from minimization of volumetric flow and makes plumbing of the delivery system somewhat simpler. The other choice has been inert gases

such as nitrogen or argon. This approach might be used if there is concern about reaction in the lines, or corrosion of the system is considered probable with the use of oxygen carrier gas.

2) The control scheme used most commonly is that shown in Figure 6, for example, as described by Nordberg (1943). In this case the quantity of carrier gas (mass or combination of pressure and volume) fed into the bubbler is controlled. Stringent control of bubbler temperature and the level of saturation is required to obtain accurate control of reactant flow. This approach incurs some variability due to changes in barometric pressure as well as variations in pressure due to piping and flow rate. A second more complex approach is the use of mass flow differential. In this method the mass of reactant and carrier flow and carrier flow alone are directly measured by thermal conductivity cells. The mass of reactant flow can be inferred by difference which then provides a feedback control loop for the carrier gas flow. In principle, this approach eliminates some level of control of temperature, pressure and saturation. It suffers, however, from having to flow potentially corrosive reactant vapor through accurate instrumentation. Commercial units providing this function do require more maintenance. Improvement in such instrumentation may spread use of this control scheme.

3) Temperature control of the liquid raw material is achieved in several ways. First, the bubblers are normally heated at least 5°C above ambient to improve control. Increased temperature also increases vapor pressure of the liquid and thereby improves saturation which can be of benefit to processing. Two alternatives used for temperature control are individual bubbler liquid temperature control and cabinet temperature control with all the bubblers having the same temperature. Controlling liquid temperature becomes more of a problem for larger bubblers, higher deposition rates, and longer run times for obvious reasons.

4) Saturation control is particularly critical if the reactant flow is controlled by flow of carrier gas upstream of the bubbler. The majority of bubblers used today consist simply of a diptube inserted close to the bottom of the bubbler, through which carrier gas is fed. An alternative is the use of saturation columns above the bubbler. A trade-off between simplicity and improved precision must be considered.

5) The material of construction of vapor delivery systems used today vary from all metallic welded construction to all non-metallic. It is well known that to use metallic systems one has to keep moisture out of the system to prevent corrosion. Technology exists to accomplish this. If one postulates that keeping moisture out is an impossible task, non-metallic glass or plastic systems are preferred. However, glass components are subject to breakage and plastic to permeation of moisture through the material.

It is not clear that the components of the vapor delivery system are the limiting factors for control of fiber tolerances or fiber properties. The variability of other process parameters is probably still larger than the variability of vapor flow, provided all control units are routinely maintained and calibrated.

There are several other systems that have been proposed as alternatives to the bubbler systems. One of these is shown in Figure 7 (Blankenship, 1979). The primary feature of this system is a metering pump which delivers liquid reactant to a temperature-controlled flask nebulizer where the gaseous reactants are added and the mixture is fed to the heat source. This approach requires a metering pump that can handle metal halides. Also, this approach does not benefit from the presence of the bubbler which serves to distill the liquid, at least initially. Another system is shown in Figure 8

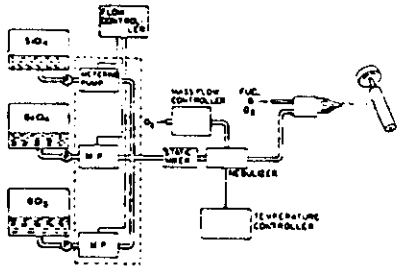

Vapor generation system using metering pumps (Blankenship, 1979).

Figure 7



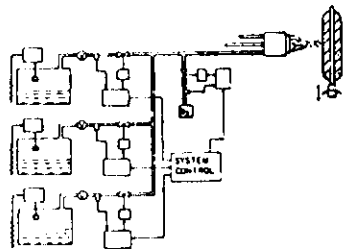

High temperature direct vapor control system (Blankenship, 1982).

Figure 8

(Blankenship, 1982a). This is a high temperature system that eliminates the need of carrier gas bubbling by using direct vaporization. This approach requires high temperature flow control devices. Both of these approaches eliminate some of the problems of the bubbler system, but have a few of their own. The kind of vapor delivery system that will become most used depends on the nature and scale of the processes of the future and improvements in capability and reliability of control devices.

## Chemical Reactions and Particle Formation

The chemical reactions involved in the formation of the glass soot are complex, involving not only the $SiCl_4$, $GeCl_4$, and $O_2$, but also the fuel gas ($CH_4$ or $H_2$) combustion products. At present it is believed that the chlorides first react with $O_2$, Equations (1) and (2), as they are heated to above 1500°C in the flame (Powers, 1978a).

$$SiCl_4 + O_2 \rightleftarrows SiO_2 + 2Cl_2 \qquad (1)$$

$$GeCl_4 + O_2 \rightleftarrows GeO_2 + 2Cl_2 \qquad (2)$$

Equation (2) is shown as being in equilibrium because $GeO_2$ is not significantly more stable than $GeCl_4$ at these temperatures.

The water from the combustion of the fuel gas reacts with chlorine to produce hydrogen chloride, Equation (3).

$$2H_2O + 2Cl_2 \rightleftarrows 4HCl + O_2 \qquad (3)$$

The effect of this reaction is to consume a large portion of the chlorine produced by the formation of $SiO_2$ and $GeO_2$. The removal of chlorine from the reaction mixture allows the reaction shown in Equation (2) to proceed further to the right resulting in the formation of more $GeO_2$. At temperatures above 1800°C, $GeO_2$ decomposes to GeO (g) as shown in Equation (4)

$$GeO_2(s) \rightleftarrows GeO(g) + \tfrac{1}{2} O_2(g) \qquad (4)$$

Competing reactions of this type make it necessary to understand all the thermodynamic and kinetic aspects of the particle formation process in order to control the composition of the deposited material.

The glass particle formation has been shown to begin within about 10 mm from the burner face and is nearly complete within 100 mm. Typically the first particles formed are on the order of 0.1 µm in diameter. These grow by collision and coalescence to produce particles up to 0.25 µm. Due to the high temperature, Equations (2)–(4) are in equilibrium, and the particles can vary in composition depending on the part of the flame in which they are formed. The extent to which particles are not homogeneous is still under investigation.

## Particle Collection

The submicron spherical glass particles produced in the OVD process vary in size throughout the flame. A scanning electron micrograph of particles collected on a target rod is shown in Figure 9. Due to the small size of the particles, they cannot be collected by impaction because they tend to follow the gas streamlines. Careful analysis of the collection of soot particles onto a porous preform indicates that thermophoresis is the dominant mechanism for collection. As the hot gas stream and glass particles go around the preform, a thermal boundary layer is set up near the preform. This boundary layer is a steep thermal gradient in which the glass particles are pushed by a thermo-

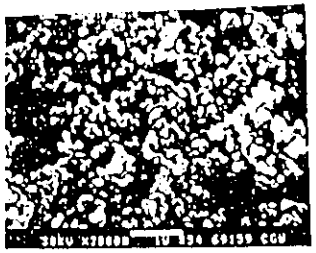

Scanning electron micrograph of OVD soot showing glass spheres.

Figure 9

phoretic force towards the preform. In studies to maximize deposition rate from a single OVD burner, it has been demonstrated (Blankenship, *et al*., 1982) that, for a given burner, two key parameters are target diameter and fuel gas flow. Figure 10 At

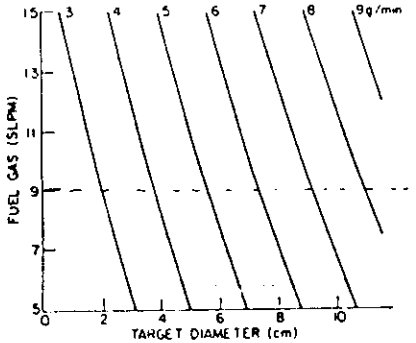


OVD deposition rate as a function of target diameter and fuel gas flow (Blankenship, *et al*., 1982).

Figure 10

larger target diameters, the circumference and surface area of the preform increase allowing more time and area during which the particles are close enough to the surface to be collected. Also, the average preform temperature is reduced. Increasing the thermophoretic force. Increasing the fuel gas flows increases the soot particle temperature and therefore the thermophoretic force. The average collection efficiency of the OVD process is around 50%

## Drying and Sintering

The process steps of drying and sintering are very similar for the OVD and the VAD processes. However, they are significantly different from the MCVD process. The published literature on drying and sintering in the VAD process covers the fundamentals of this process step extensively (Edahiro, *et al*., 1980). Only the basic differences in the drying process between the OVD and VAD processes will be discussed in order to avoid duplication and because many aspects of this process step are proprietary.

Perhaps the most significant difference is in the way drying gases are fed into the preform within the furnace environment. In the OVD process, the removal of the target rod makes it possible to deliver the drying gases through this centerhole as the preform is fed down through the sintering furnace (Powers, 1978b). This is shown in Figure 11. Although the elimination of all hydroxyl ions from the preform is attempted, the radial hydroxyl ion gradient, if any, is favorable for propagation of light in the core of the fiber when this approach is used. This hydroxyl ion gradient is shown schematically compared to that of the VAD process in

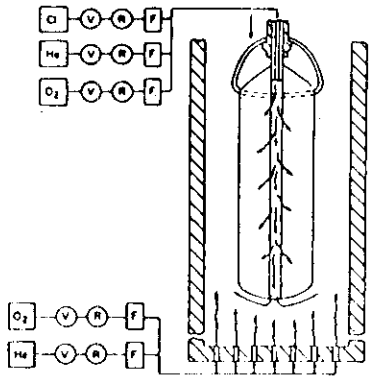


Drying of an OVD perform through the centerhole (Powers, 1978b).

Figure 11



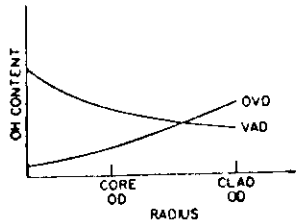


Hydroxyl gradient for OVD and VAD processes versus radius.

Figure 12

Figure 12. This is considered to be an important feature of the OVD process that has made it possible to obtain the level of drying in OVD fibers shown in Figure 25 of this paper. There is little difference in the sintering of VAD and OVD preforms. A theoretical analysis of the kinetics of sintering has been reported by Scherer (1977).

## OVD Preform Design

An added complexity in fabricating multimode fibers in particular using the OVD process is that of preform fracture due to thermal shock. This occurs because most dopants increase the thermal expansion coefficient of the glass. Thus, in graded index fibers, the maximum tensile stress is at the centerhole. Furthermore, removal of the target rod can easily leave defect sites on the centerhole. The above combination was a major cause of preform breakage after consolidation in early development efforts.

The breakage problem can be addressed by at least four different approaches. The first is a conventional solution based on simple physical principles (Blankenship, 1982). A low expansion layer is deposited on the centerhole surface such that it is in compressive stress. If the defect sites are shallower than the compressive layer thickness, crack propagation is refracted. This is schematically shown in Figure 13.

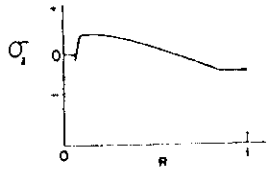


Stress profile produced using low expansion centerhole layer (Blankenship, 1982b).

Figure 13

The second approach is to balance the expansion coefficient of the core with that of the cladding such that the stress at the centerhole is much reduced or eliminated (Gulati and Scherer, 1982). This can be done conveniently using $B_2O_3$ as a dopant because $B_2O_3$ reduces the index of $SiO_2$ while increasing its thermal expansion coefficient. Therefore, the stress effects of $B_2O_3$ and $GeO_2$ can be balanced at no cost in index differential between core and clad. Due to the infrared absorption edge of $B_2O_3$, however, this approach is only useful for fibers operating at wavelengths below about 1.2 μm. Typical expansion coefficient gradients of stress-balanced and uncompensated designs are shown in Figure 14.

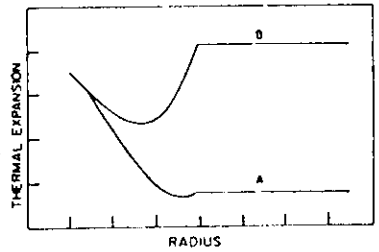


Comparison of thermal expansion coefficient profiles for uncompensated (A) and stress-balanced (B) designs.

Figure 14

A third approach is to control the density and compositional gradients within the porous preform such that the hole closes during the consolidation process step, thereby eliminating the centerhole as a defect site in the high expansion area (Blankenship, 1981). Theoretical analysis (Scherer, 1979)

and successful use of this approach have been reported. A low viscosity glass layer on the center hole has been shown to promote seedfree hole closing when this approach is used (Bailey and Morrow, 1983).

A fourth approach which not only eliminates this problem but also improves process productivity is shown in Figure 15 (Bailey, 1979). In this case the

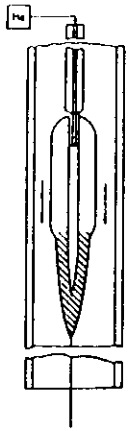

Schematic of combined consolidation and draw process (Bailey, 1979).

Figure 15

consolidation process step is combined with fiber drawing such that the sintered glass does not have the opportunity to cool down below the glass transition temperature prior to being drawn into fiber. This prevents stress formation thereby eliminating breakage.

## OVD Fibers and Their Performance Characteristics

At the present time there are three general classes produced by the outside deposition process. They are, i) single-mode fiber, ii) multimode graded index fiber for long-distance communication systems, and iii) large-core multimode graded index fiber for high capacity short-distance data transmission systems. The rest of this section is devoted to describing the performance characteristics of these fibers.

## OVD Single-Mode Fibers

The OVD single mode fibers developed to date include a step-index profile $GeO_2$-$SiO_2$ core, $SiO_2$ clad fiber optimized for operation at the 1.3 μm wavelength range. The attenuation distribution of recent production fibers at 1.3 μm is shown in Figure 16. The associated hydroxyl ion content

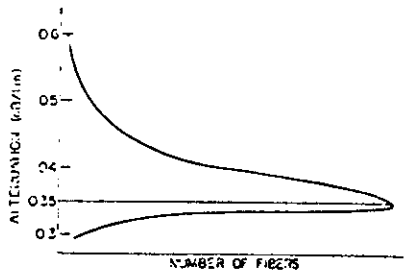


OVD single-mode fiber attenuation distribution.

Figure 16

distribution is shown in Figure 17. The hydroxyl ion content was computed from the attenuation spectrum assuming 100 ppb $OH^-$ content causes an absorption peak of 3.3 dB/km at 1.39 μm. In single-mode fibers, scattering coefficient is wavelength dependent (Bhagavatula, *et al.*, 1983a). It is a function of the composition of the core and cladding glasses as well as the power distribution between the core and cladding. The scattering behavior of OVD single-mode fibers has been characterized by direct scattering measurements and a typical behavior is shown in Figure 18. A typical refractive index profile obtained for OVD single mode fibers is shown in Figure 19. Concentricity of the core in the fiber is an important parameter if power optimization is not done during splicing. State-of-the-art measurement techniques have been instituted to quantitatively measure this parameter. A typical distribution is shown in Figure 20.

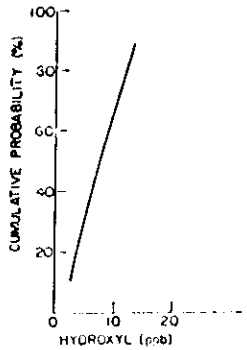


OVD single-mode fiber hydroxyl distribution.

Figure 17

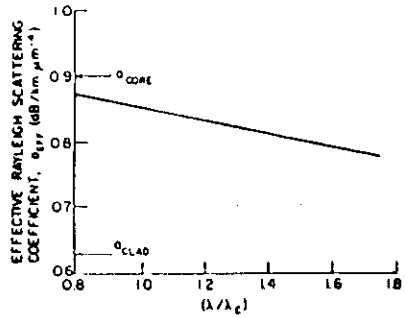


OVD single-mode fiber scattering behavior (Bhagavatula, *et al.*, 1983a).

Figure 18

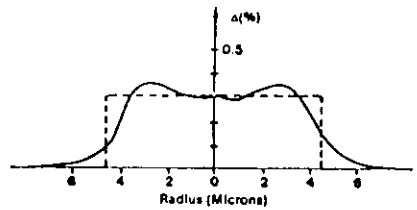


OVD single-mode fiber refractive index profile.

Figure 19

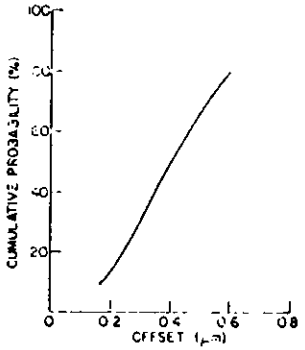


OVD single-mode fiber core offset distribution.

Figure 20

The dispersion requirements on single-mode fibers are more stringent due to mode partition noise of conventional single-mode laser diodes. OVD single-mode fibers have been designed to operate over 35 km lengths at up to 405 Mbits data rate in conjunction with conventional 1.3 μm single-mode laser diodes having spectral widths of 4 nm. Another design criterion was that attenuation up to 1.55 μm wavelength could not be significantly affected by bending or microbending due to cabling. It is understood, however, that for higher bit rate systems within this wavelength range, improvements will have to come in the laser performance if this fiber design is to be employed.

To ensure this level of performance, the normalized refractive index difference, Δ, and the effective cut-off wavelength of the fiber are tightly controlled to

nominal values of 0.3% and 1.2 μm respectively. The dispersion when these parameters are held within the specified tolerances is less than 3.5 psec/nm·km over the range from 1.285 to 1.33 μm as shown in Figure 21. Extensive cabling trials using

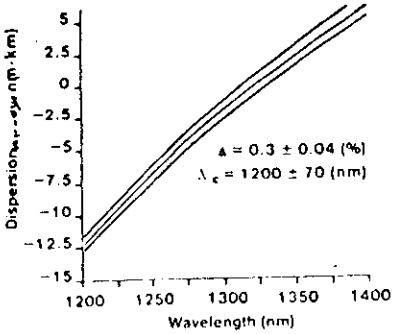


OVD single-mode fiber dispersion versus operating wavelength.

Figure 21

loose tube construction have verified the soundness of the design with respect to cabling-induced bending and microbending loss. Trial installations using conventional lasers have shown that the bit error rate of systems are well within design limits, even though some fibers may indeed be overmoded (i.e., the theoretical V-value may be greater than 2.4 using equivalent step parameters for the computation) at the operating wavelength. The actual dispersion level necessary and size of the wavelength range required for operation is expected to evolve with experience. Improved process control in both laser and fiber manufacturing will help optimize system performance.

In order to take advantage of the lower attenuation at the 1.55 μm wavelength without the need for narrow spectral width lasers to achieve high bit rates, fibers are being designed with minimum dispersion, $\lambda_{o_1}$ shifted to this wavelength. This is possible because the material dispersion stays relatively constant in silica fibers but the waveguide dispersion can be adjusted by changing index profile and Δ. Total or chromatic dispersion is the sum of these two terms. Fibers having excellent attenuation, dispersion, and microbending insensitivity have been made by the OVD process with designs as shown in Figure 22 (Bhagavatula, *et al.*, 1984). Using more complicated designs such as are shown in Figure 23 (Bhagavatula, *et al.*, 1983b) it is possible to achieve low dispersion over a wider wavelength range, for example less than 2 psec/nm·km over the range from 1.3 to 1.6 μm. OVD fibers having these types of designs are expected to be developed and in production when required by systems.

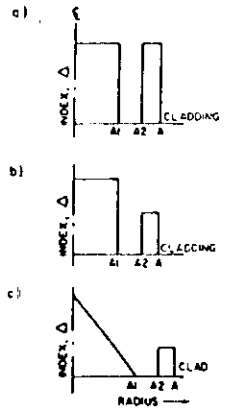


SEGCOR™ dispersion-shifted single-mode designs (Bhagavatula, *et al.*, 1984).

Figure 22

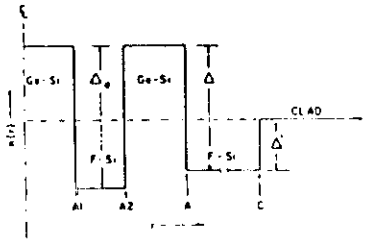


SEGCOR™ dispersion-flattened single mode designs (Bhagavatula, *et al.*, 1983b).

Figure 23



## OVD Long-Distance Graded Index Multimode Fibers

In multimode fibers the primary focus in the recent past has been in increasing process understanding and process control to improve fiber performance. This has to be done in conjunction with process and equipment innovation programs and automation efforts to improve productivity of the process. These two basically conflicting efforts, have sometimes helped and sometimes impeded improvement in fiber characteristics.

The most remarkable progress has been in improvement in attenuation characteristics shown in Figure 24. One of the most significant

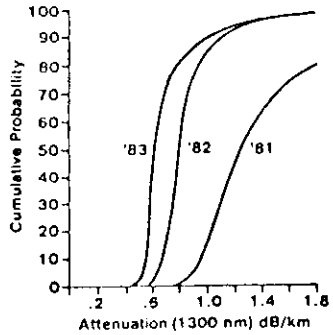


OVD multimode fiber attenuation distribution (all fiber/typical line).

Figure 24

contributors to this improvement has been the ability to reduce and control the level of hydroxyl ion content in the fiber, shown in Figure 25.

Another significant improvement in the OVD process has been in the understanding of bandwidth control of individual fibers and of concatenated lengths. Several papers have been presented in recent conferences on this topic (Love, 1982 and 1983). The key findings of these studies are summarized below.

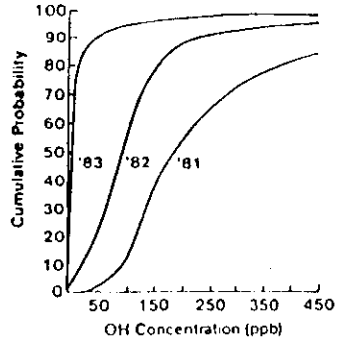


OVD multimode fiber hydroxyl distribution (all fiber/typical line).

Figure 25

Extensive analysis of pulse broadening in multimode fibers leads to the conclusion that the pulse broadening, σ, of a fiber is a function of length, L, and wavelength, λ, and can be expressed as follows:

$$\sigma^2(L,\lambda) = \sigma_m^2(\lambda)L^2 + \sigma_\delta^2(\lambda)L^2 + \left[\sigma_\xi^2(\lambda)L^2 + \sigma_\alpha^2(\lambda)L\right]_{P=1} \qquad (5)$$

where $\sigma_m$ and $\sigma_\delta$ are the pulse broadening due to material dispersion and profile error respectively and the third term is due to radial and longitudinal perturbations in the index profile. These perturbations are found to be of two types. Some are correlated, i.e., appear to be invariant along the length of the fiber (for example the curvature in the core-clad interface in the refractive index profile shown in Figure 26). Others are random in nature. The pulse broadening due to these two kinds of perturbations, $\sigma_\xi$ (correlated) and $\sigma_\alpha$ (uncorrelated or random), have different length dependence.

It is interesting to note that in the OVD process, at the wavelength where the profile exponent, α, is optimum, pulse broadening is proportional to the square root of length within a unit length of fiber. This was determined by cutting back a unit length of fiber and measuring fiber bandwidth as a function of wavelength. At the wavelength where α is optimum or where the fiber bandwidth is maximum,

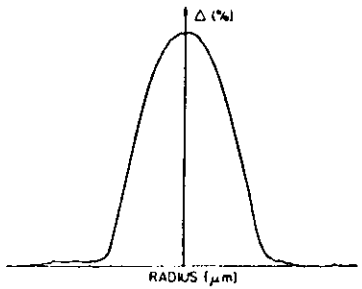


OVD multimode fiber refractive index profile.

Figure 26

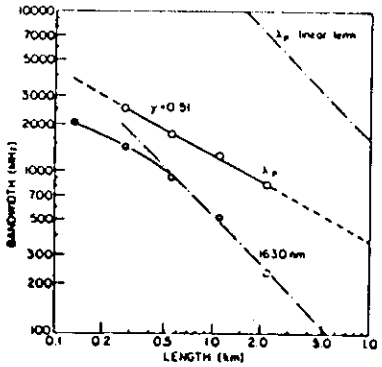


Length dependence of bandwidth at the optimum wavelength ($\lambda_p$) and away from optimum (1630 nm) (Love, 1982).

Figure 27

the length dependence of bandwidth is shown in Figure 27 (Love, 1982). The implication of this observation is that in the context of the measured fiber lengths, the index perturbations in OVD fibers are uncorrelated. It is then not surprising that when fibers with optimum α at the measured wavelength are concatenated, in OVD fibers, the length dependence of bandwidth has the same functional dependence. This is shown in Figure 28 (Love, 1983).

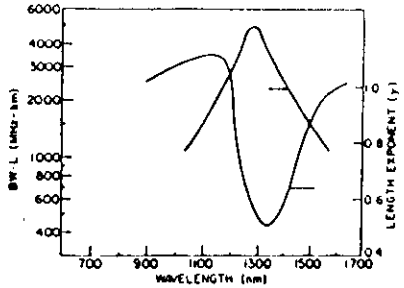


Concatenated bandwidth-length product and length exponent (γ) versus wavelength (λ) for OVD fiber (Love, 1983).

Figure 28

In spite of this extremely favorable length dependence of bandwidth and championship results of 3-4 GHz·km measured on 2.2 km lengths, fiber bandwidth has not been controlled to the level desired. The primary reason for this is the rate of change imposed on the process to improve productivity. Figure 29 shows the changes in

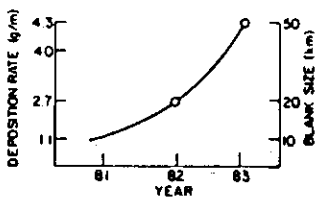


OVD deposition rate and blank size progress by year.

Figure 29

deposition rate and preform size which have been made in the last three years. Another factor that impedes bandwidth performance is the complexity imposed on the process by the need to prevent cracking of the preform due to stresses at the centerhole after the preform is consolidated. The existing OVD process capability in producing high bandwidth multimode graded index fiber is shown in Figure 30. In the near future, significant improvement of the bandwidth distribution is likely



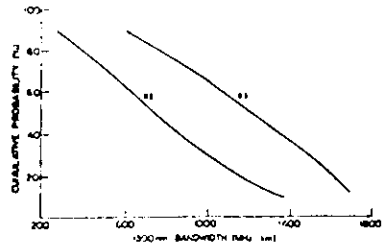


OVD multimode fiber bandwidth distribution (all fiber/ typical line).

Figure 30

## OVD Short-Distance Fibers

Short-distance fibers have now been designed for application in high capacity data links, where the quasi-step ($\alpha \geq 3.5$) ≤ 50 MHz·km fibers previously developed (Morrow, *et al*., 1979) are considered inadequate. In addition to the above, the fiber is designed to operate at both the 0.85 μm and 1.3 μm wavelength ranges, as described by Jones and Sommer (1982). The fiber design is a graded index multimode fiber with nominally 0.29 NA and dimensions of 100 μm core diameter and 140 μm fiber diameter. The large core diameter and the relatively high NA are required to maximize coupling of light power into the fiber from LEDs. The proneness to cabling loss due to microbending in this design is significantly improved over standard long-distance multimode fibers and therefore not considered a key factor. In addition, since the intended applications use short links and are expected to be highly connectorized, the increased fiber cost due to increased diameter and higher germania content is felt to be well justified by reduced total system cost.

A typical refractive index profile of such a fiber is shown in Figure 31. The index depression at the axis of the fiber is due to the design and is not a feature of the OVD process. Typical attenuation distributions of the fiber at 0.85 and 1.3 μm are shown in Figure 32. The increased attenuation of 0.85 μm is due to the increased Rayleigh scattering coefficient of the design. The high attenuation level

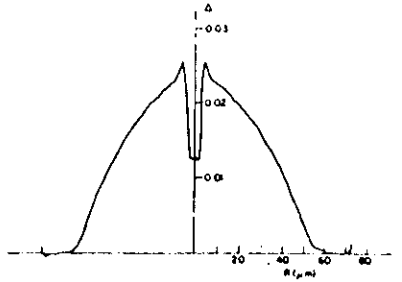


OVD short-distance fiber refractive index profile (Jones and Sommer, 1982).

Figure 31

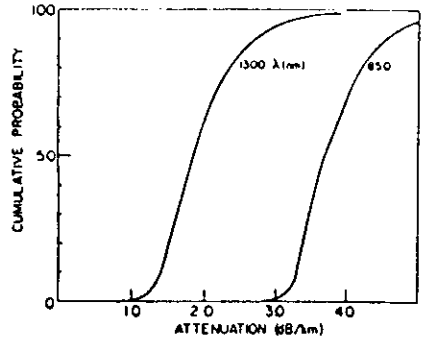


OVD short-distance fiber attenuation distribution.

Figure 32

at 1.3 μm is due to the fact that relatively little attention has been given to the hydroxyl ion content of this fiber. The attenuation levels shown here are considered adequate for the application. Since these fibers are designed to operate at both 0.85 μm and 1.3 μm simultaneously the bandwidth of the fiber is peaked at a wavelength in between. Typical bandwidth distributions of such fibers at both wavelengths are shown in Figure 33.

Other fiber designs to serve related applications are now in development. For example, a fiber design which is expected to be more advantageous for local area network applications has a

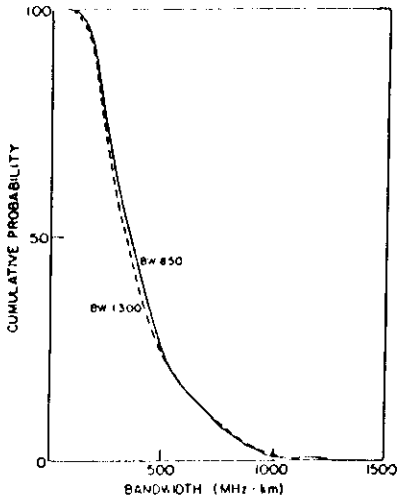


OVD short-distance fiber bandwidth distribution.

Figure 33

0.26 NA, 85 µm core, and 125 µm fiber diameter with similar or better bandwidth and attenuation to the short-distance fiber described above. The flexibility of the OVD process makes large-core, high-NA fibers such as these relatively easy to fabricate compared to VAD and MCVD processes where tubes are often used for cladding.

New Developments and Summary

This section has been created to provide a glimpse into what is expected to happen in OVD in the near future. The information is not complete being composed primarily of early results of development activities.

A significant new development is the ability to incorporate fluorine into OVD fibers without the aid of plasma torches as well as the ability to retain this fluorine and at the same time dry the fiber (Berkey, 1984). Figure 34 shows a typical refractive index profile of a silica-core fluorosilicate-clad single-mode fiber. The ability to incorporate fluorine also helps in fabricating high NA multimode fibers. The result of one such attempt is shown in Figure 35

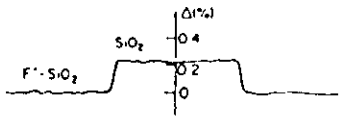


Silica-core fluorosilicate clad refractive index profile (Berkey, 1984).

Figure 34

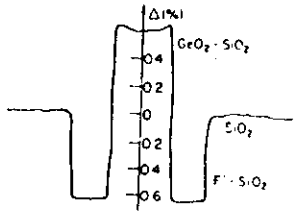


Refractive index profile of high NA step index fiber with fluorine-doped clad (Berkey, 1984).

Figure 35

Progress is also being made in research for other new dopant materials. A new family of materials has been developed which may permit successful use in the OVD process of many more dopants than have previously been available in high vapor pressure liquids form. The thrust has been aimed at reduction of Rayleigh scattering, enhancing the extent of refractive index change per unit change in expansion coefficient due to doping (for high NA fibers), improving radiation hardness of low loss fibers, and in developing fibers for longer wavelength operation. The OVD and VAD processes have an advantage over MCVD in this area because dopants containing hydrogen may be used. This is true because the sintering and drying steps are separate from deposition in these processes.

A third area of new product development that has shown exceptional progress has been in the area of high birefringence polarization retaining single-mode fibers (Marrone, *et al.*, 1984). Figure 36 shows a cross-section of a design for such fiber.



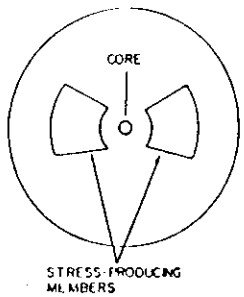


Design for polarization-retaining single-mode fiber (Marrone, *et al.*, 1984).

Figure 36

Typical performance characteristics of these fibers are attenuation at 0.85 µm of 3.4 dB/km, beat length of about 2 mm, and extinction ratio of greater than 18 dB using a broad spectral source.

In summary, the OVD process is now a fully industrialized and automated manufacturing process. It is the primary process used in Corning's optical fiber manufacturing plant in Wilmington, N.C. The process has been scaled up so that preforms of ≥ 50 km in size can now be routinely produced. Average deposition rates of greater than 4 gm/min have been achieved. Fiber designs ranging from single-mode to large-core multimode have been successfully made in production. The flexibility of the process is being constantly exploited to produce fibers of diverse designs and compositions to meet the ever-expanding needs for optical fibers. Recent examples are new single-mode designs, fiber for local-area-network applications, and polarization-retaining fibers.

Although the rate of progress has been close to incredible, there is much in a process as complex as the OVD process still to be learned. Because of its flexibility, high rate, and ability to use new dopants, its potential is great for being able to provide the high-quality fiber and glass needed in the future, both for optical communications and for applications yet to be discovered.

References


1. Bailey, A. C. (1979) U.S. Patent 4,157,906.
2. Bailey, A. C. and Morrow, A. J. (1983) U.S. Patent 4,413,882.
3. Barns, R. L., Chandross, E. A., and Melliar-Smith, C. M. (1980) In "Proc. 6th European Conf. Opt. Commun.", (York, U.K.), 26-28.
4. Berkey, G. E. (1984) In "Tech. Dig., Conf. Opt. Fiber Comm.", (Optical Society of America, Wash.) paper MG3.
5. Bhagavatula, V. A., Berkey, G. E., and Sarkar, A. (1983a) In "Tech. Dig., Topical Mtg. Opt. Fiber Comm.", (Optical Society of America, Wash.), 22-25.
6. Bhagavatula, V. A., Spotz, M. S., Love, W. F., and Keck, D. B. (1983b) *Electronics Letters 19*, 317-318.
7. Bhagavatula, V. A., Spotz, M. S., and Quinn, D. E. (1984) In "Tech. Dig., Conf. Opt. Fiber Comm.", (Optical Society of America, Wash.), paper MG2.
8. Blankenship, M. G. (1979) U.S. Patent 4,173,305.
9. Blankenship, M. G. (1981) U.S. Patent 4,251,251.
10. Blankenship, M. G. (1982a) U.S. Patent 4,314,837.
11. Blankenship, M. G. (1982b). U.S. Patent 4,344,670.
12. Blankenship, M. G., Morrow, A. J., and Silverman, L. A. (1982) In "Tech. Dig., Topical Mtg. Opt. Fiber Comm.", (Optical Society of America, Wash.), 18-19.
13. Dumbaugh, W. H. and Schultz, P. C. (1975). U.S. Patent 3,864,113.
14. Edahiro, T., Kawachi, M., Sudo, S., and Inagaki, N. (1980) *Rev. Electrical Commun. Lab., NTT 27*, 58-68.
15. Gulati, S. and Scherer, G. W. (1982) U.S. Patent 4,358,181.
16. Hyde, J. F. (1942). U.S. Patent 2,272,342.
17. Jones, P. C. and Sommer, R. G. (1982) In "Tech. Dig., Topical Mtg., Opt. Fiber Comm.", (Optical Society of America, Wash.), 20-21.
18. Kapron, F. P., Keck, D. B., and Maurer, R. D. (1970). *Appl. Phys. Lett. 17*, 423-425.
19. Love, W. F. (1982). In "Tech. Dig., Topical Mtg. Opt. Fiber Comm.", (Optical Society of America, Wash.), 26-27.
20. Love, W. F. (1983). In "Tech. Dig., Topical Mtg. Opt. Fiber Comm.", (Optical Society of America, Wash.), 64-67.
21. Marrone, M. J., Rashleigh, S. C., and Blaszyk, P. E. (1984). To be published in *J. Lightwave Tech.*
22. Morrow, A. J., Sommer, R. G., Keck, D. B., and Gunderson, L. C. (1979) In "Tech. Dig., Topical Mtg. Opt. Fiber Comm.", (Optical Society of America, Wash.), 66-67.
23. Nordberg, M. E. (1943). U.S. Patent 2,326,059.
24. Powers, D. R. (1978a). *J. Amer. Ceram. Soc. 61*, 295-297.
25. Powers, D. R. (1978b). U.S. Patent 4,125,388.
26. Randall, E. N. (1975a). U.S. Patent 3,883,336.
27. Randall, E. N. (1975b). U.S. Patent 3,923,484.
28. Scherer, G. W. (1977). *J. Amer. Ceram. Soc. 60*, 236-246.
29. Scherer, G. W. (1979). *J. Non-Cryst. Solids. 34*, 239-256.
30. Schultz, P. C. (1975). U.S. Patent 3,859,073.




# MAIN ADVANTAGES OF OPTICAL FIBERS

- SMALL CABLE SIZE
- REDUCED WEIGHT
- LOW DUCT OCCUPANCY
- NO CROSSTALK
- IMMUNITY TO INTERFERENCES
- COMPLETE ELECTRICAL INSULATION
- VERY LARGE INFORMATION BW
- VERY LARGE REPEATER SPACINGS

TYPICAL OPTICAL FIBRE STRUCTURE

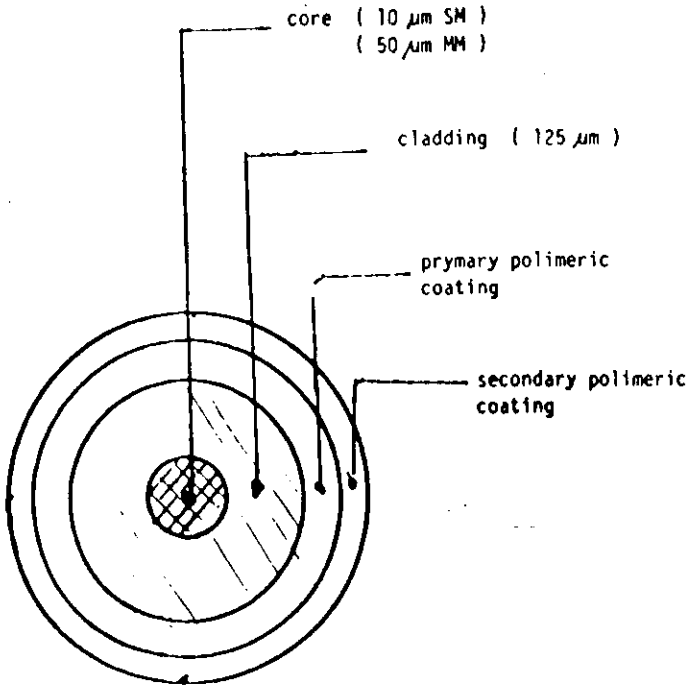


# METHODS OF PREPARING EXTREMELY PURE GLASSES FOR OPTICALS FIBERS

- CONVENTIONAL GLASS REFINING TECHNIQUES
  - GIVE RISE TO
    - STRATIFIED MELT PROCESS
    - DOUBLE CRUCIBLE METHOD
    - (.. AND MORE)
- VAPOUR PHASE DEPOSITION
  - GIVE RISE TO
    - CVD
      - IVPO
        - MCVD
        - PCVD
      - OVPO
        - OVD
        - VAD

# MAIN ADVANTAGES OF THE VAPOUR PHASE DEPOSITION METHODS COMPARED TO THE DOUBLE CROUCIBLE METHOD

- LONGER LENGTHS.
- HIGHER PRODUCTIVITY.
- HIGHER RESOLUTION IN THE REFRACTIVE-INDEX PROFILES.
- STABLER TRANSMISSION CHARACTERISTICS OF THE FIBER.
- LOWER ATTENUATION DUE TO THE HIGHER PURITY OF THE MATERIALS.

ATTENUAZIONE INTRINSECA DELLA SILICE

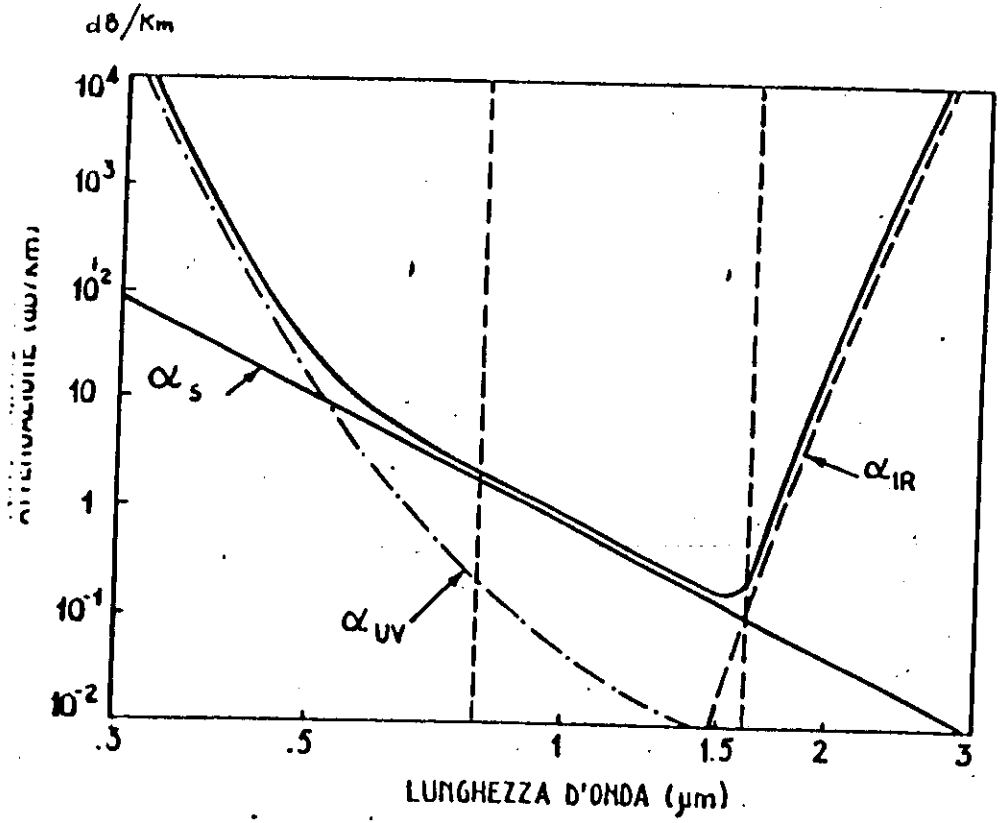

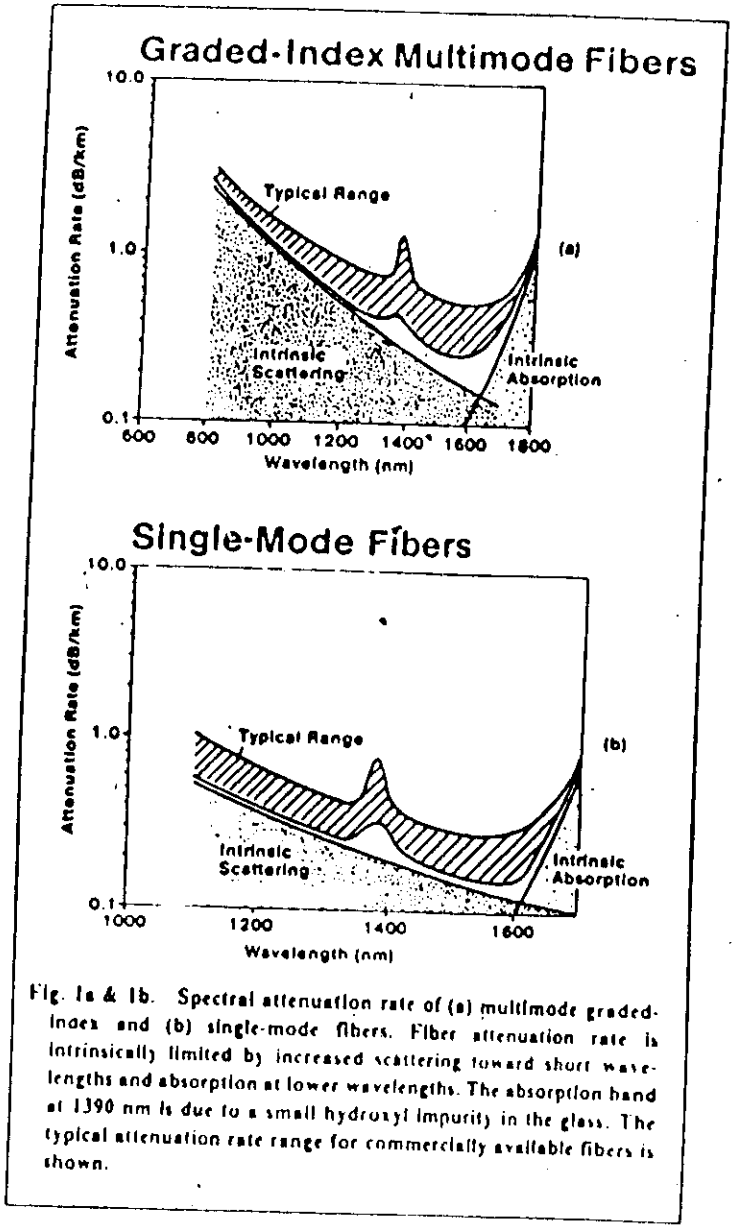


Fig. 1a & 1b. Spectral attenuation rate of (a) multimode graded-index and (b) single-mode fibers. Fiber attenuation rate is intrinsically limited by increased scattering toward short wavelengths and absorption at lower wavelengths. The absorption band at 1390 nm is due to a small hydroxyl impurity in the glass. The typical attenuation rate range for commercially available fibers is shown.

Fig. 1 bis.

Tabella 1

MECCANISMI DI ATTENUAZIONE NELLE FIBRE OTTICHE

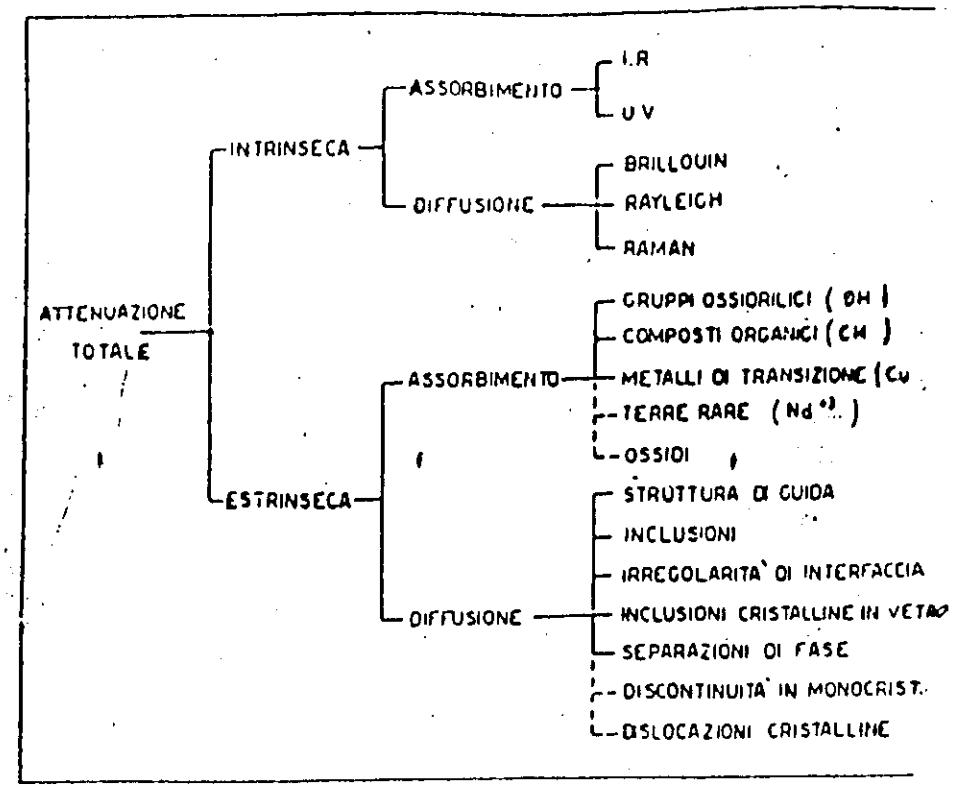

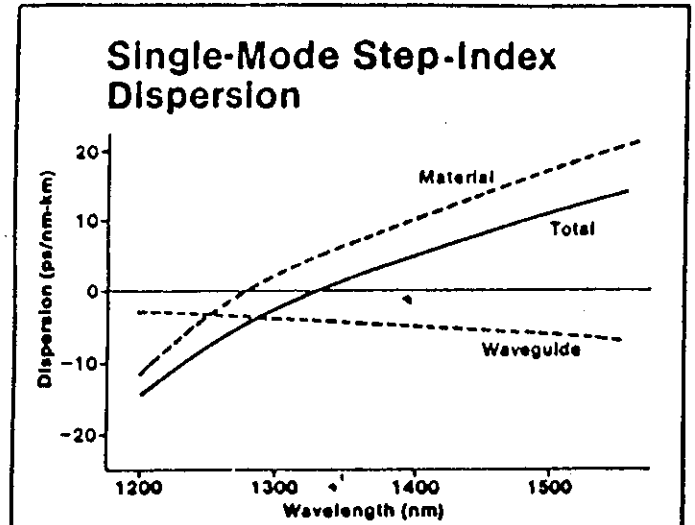


**Fig. 4. The total dispersion of single-mode fibers is a combination of material and waveguide dispersion. This produces a zero-dispersion point near 1330 nm where extremely large bandwidth is possible.**

Fig. 4 Tris

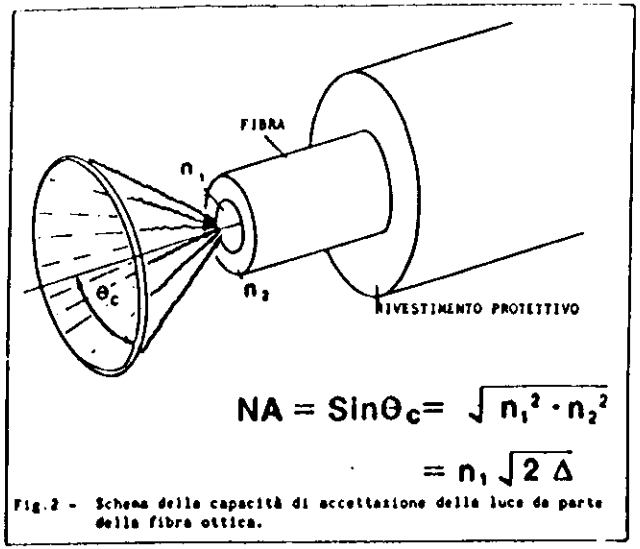


Fig.2 - Schema della capacità di accettazione della luce da parte della fibra ottica.

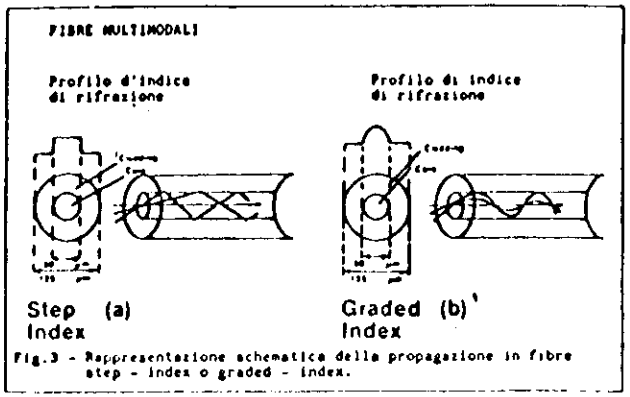


Fig.3 - Rappresentazione schematica della propagazione in fibre step - index o graded - index.

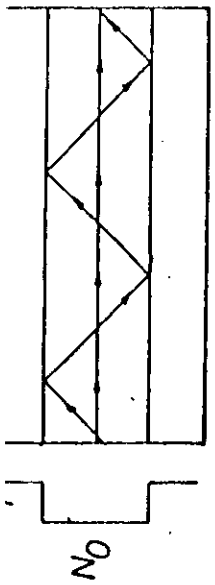


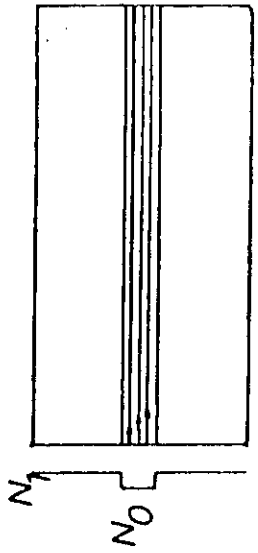


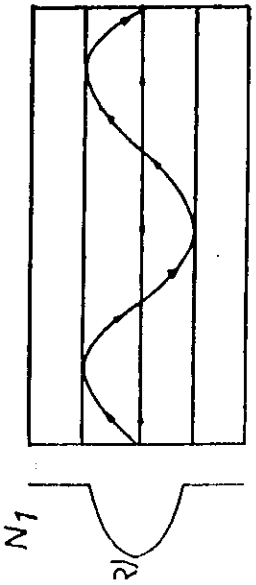


## FIBRE MONOMODALI

| PROFILO | TIPO | ATTENUAZIONE [dB/km] 1.3μm - 1.5μm | $\lambda_0$ [μm] | COMPOSIZIONE CLADDING/CORE (MAT. ALTERNATIVI) |
|---|---|---|---|---|
| | Step Index | 0.27 - 0.16 | 1.3 | $SiO_2 - GeO_2/SiO_2$ $(P_2O_5/GeO_2 - P_2O_5 - F)$ |
| | Depressed Index Cladding | 0.28 - 0.16 | ≃ 1.3 | $SiO_2 - GeO_2/SiO_2 - F$ $(P_2O_5/P_2O_5)$ |
| | « W » | 0.35 - 0.2 | 1.55 | $SiO_2 - GeO_2/SiO_2 - F$ $(P_2O_5/P_2O_5)$ |
| | Triangular | 0.37 - 0.21 | 1.55 | $SiO_2 - GeO_2/SiO_2$ (F) $(P_2O_5/GeO_2 - P_2O_5)$ |
| | Multiple Index/ Triangular | 0.45 - 0.25 | 1.55 | $SiO_2 - GeO_2/SiO_2 - (F)$ $(P_2O_5/GeO_2 - P_2O_5)$ |
| | Multiple Index/ Segmented Core | 0.4 - 0.4 | 1.3; 1.55 | $SiO_2 - GeO_2/SiO_2 - (F)$ $(P_2O_5/GeO_2 - P_2O_5)$ |
| | Pure Silica Core | 0.30 - 0.16 | 1.29 | $SiO_2/SiO_2 - F$ $(P_2O_5 - F/P_2O_5)$ |

Experiment : STEP INDEX PRODUZIONE

Fibre Name : 0421055562502

Comment : MISURA DI R.N.F. F.O.S.

| Measurement N(r) X Axis |

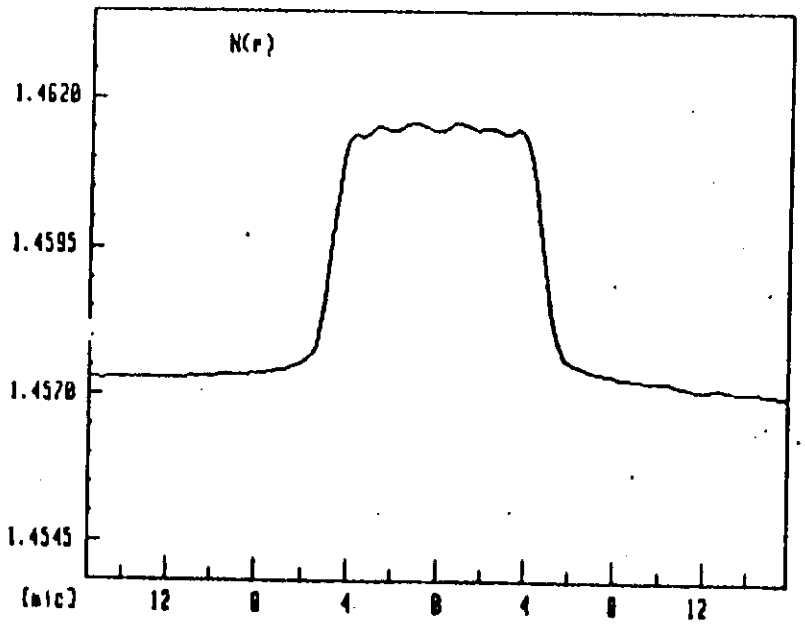


Measurement done the 03-12-1987 by PANNULLO ALFONSO



Experiment : MONOMODO TRIANGOLARE SHIFTED

Fibre Name : 211145321303

Comment : MESURAMENT OF R.N.F. F.O.S.

| Measurement N(r) Y Axis |

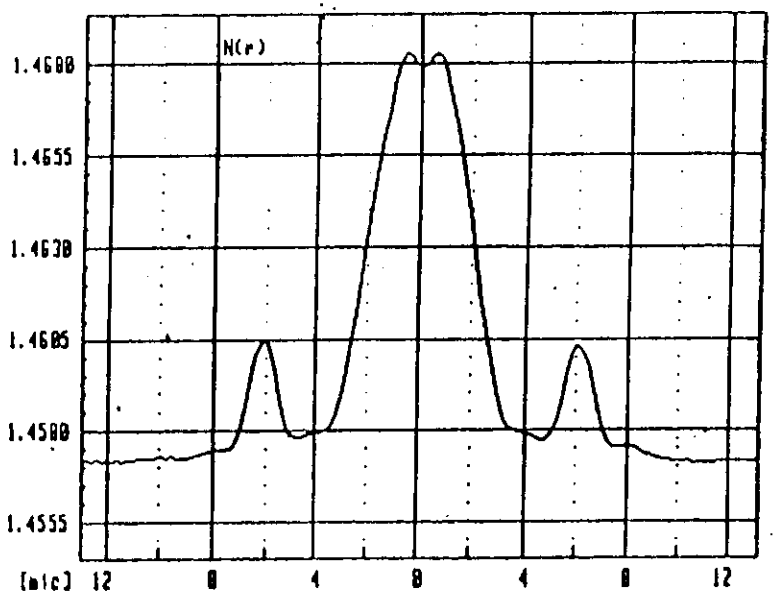

TIPICAL FIBRE COMPOSITIONS

| mantello | nucleo |
|---|---|
| $SiO_2$ | $SiO_2$-$GeO_2$ |
| $SiO_2$-(F) | $SiO_2$-$GeO_2$ |
| $SiO_2$-(F) | $SiO_2$ |

MAIN REACTIONS

$$SiCl_4 + O_2 \rightleftarrows SiO_2 + 2Cl_2\uparrow .$$
$$GeCl_4 + O_2 \rightleftarrows GeO_2 + 2Cl_2\uparrow .$$
$$CCl_2F_2 + O_2 \rightleftarrows F_2\uparrow + Cl_2\uparrow + CO_2\uparrow .$$
$$2BCl_3 + 3/2O_2 \rightleftarrows B_2O_3 + 3Cl_2\uparrow .$$
$$2POCl_3 + 3/2O_2 \rightleftarrows P_2O_5 + 3Cl_2\uparrow .$$

COMPOUNDS, BASE REAGENTS AND RELATED TEMPERATURES

TABELLA II - *Composti, reagenti di base e relative temperature.*

| Composto | TF (°C) | TE (°C) | Reagente | TF (°C) | TE (°C) |
|---|---|---|---|---|---|
| $SiO_2$ (*) | 1713 | 2230 | $SiCl_4$ | - 70 | 57.6 |
| $GeO_2$ (**) | 1086 | — | $GeCl_4$ | - 49.5 | 84 |
| $F_2$ | - 219.6 | - 188 | $CCl_2F_2$ | - 155 | - 29 |
| | | | $CF_4$ | - 184 | - 128 |
| | | | $SiF_4$ | - 90 | - 86 |
| | | | $SF_6$ | - 50.5 | 63.8 |

OPTICAL FIBRES PRODUCTION CYCLE

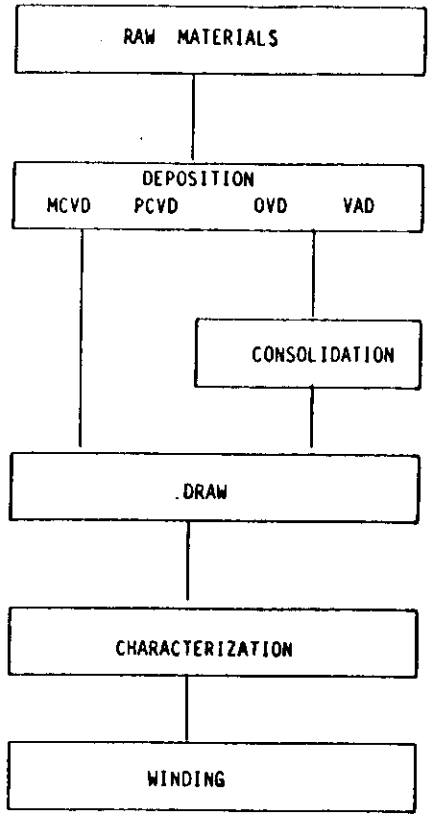


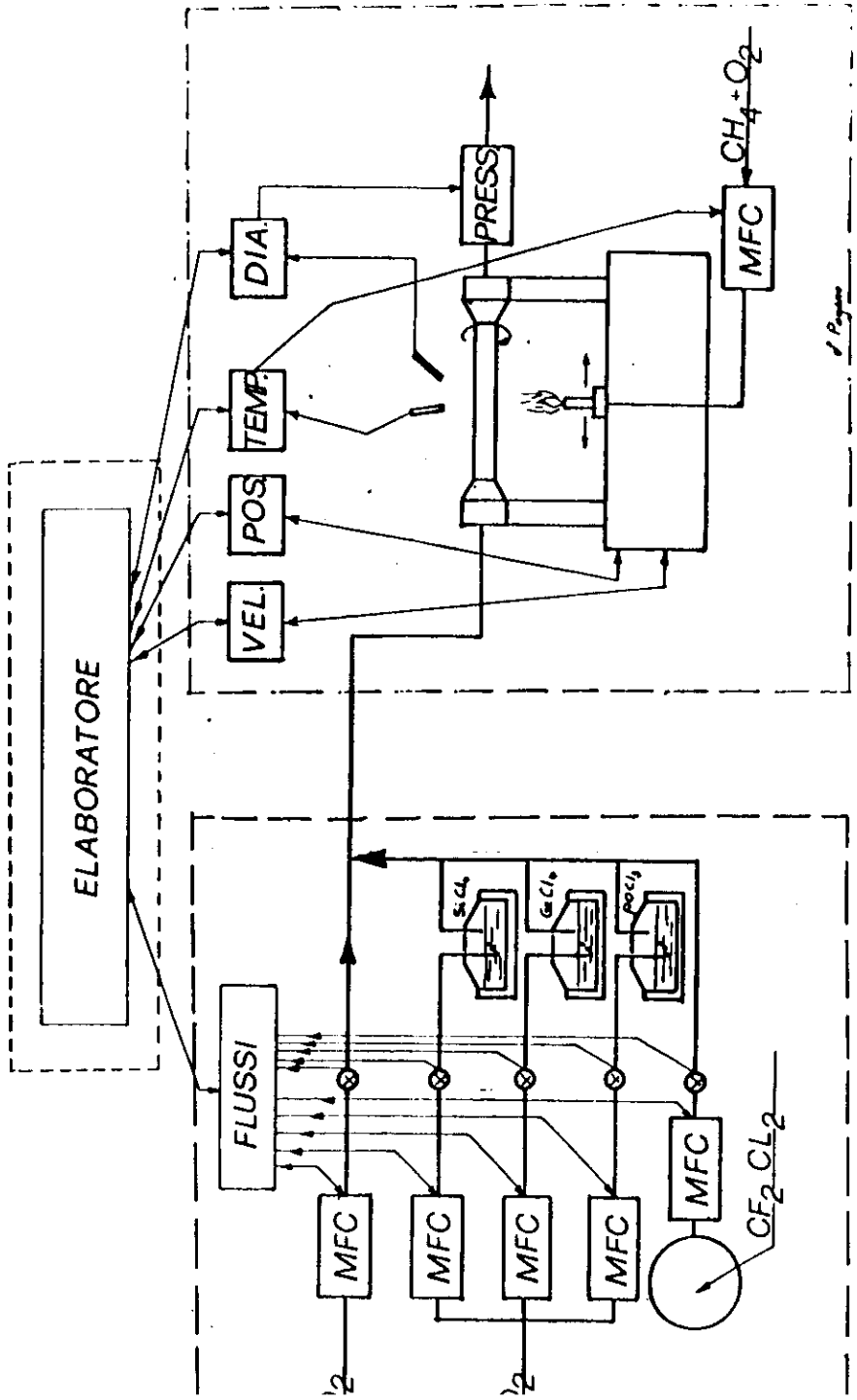

# SCHEMA PROCESSO I.V.D.

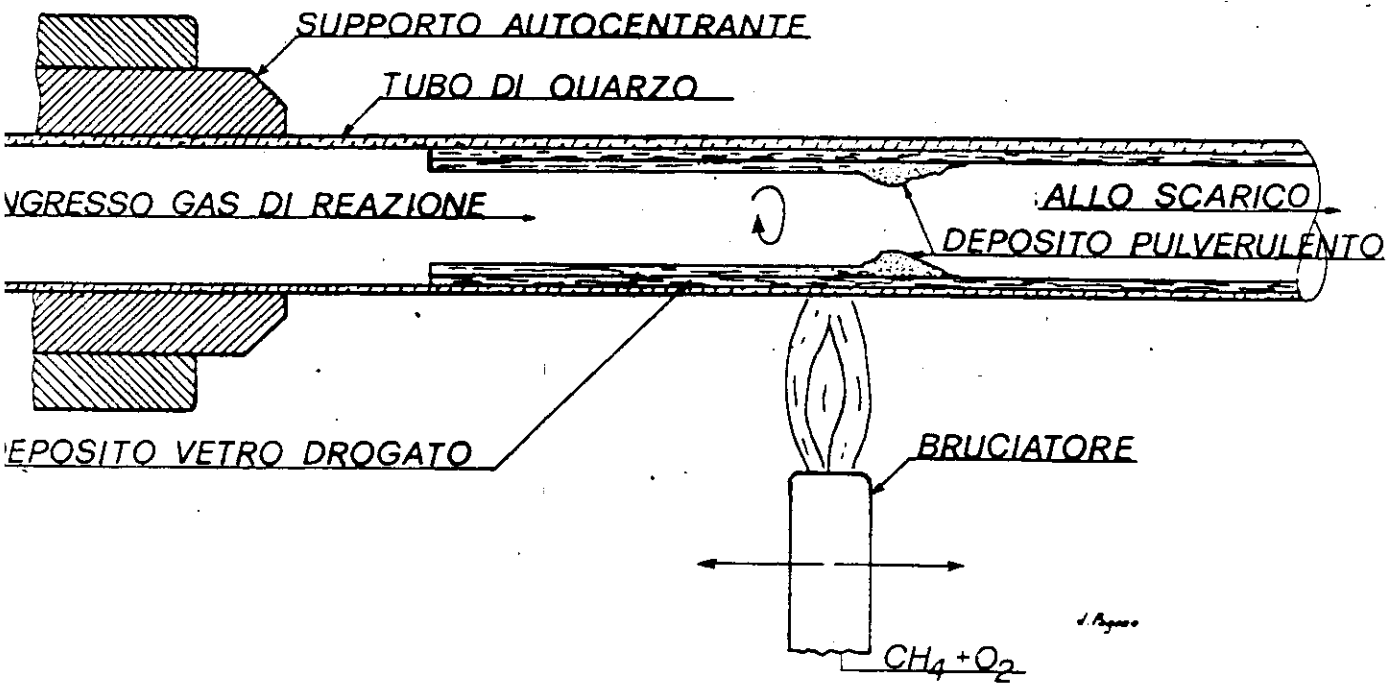


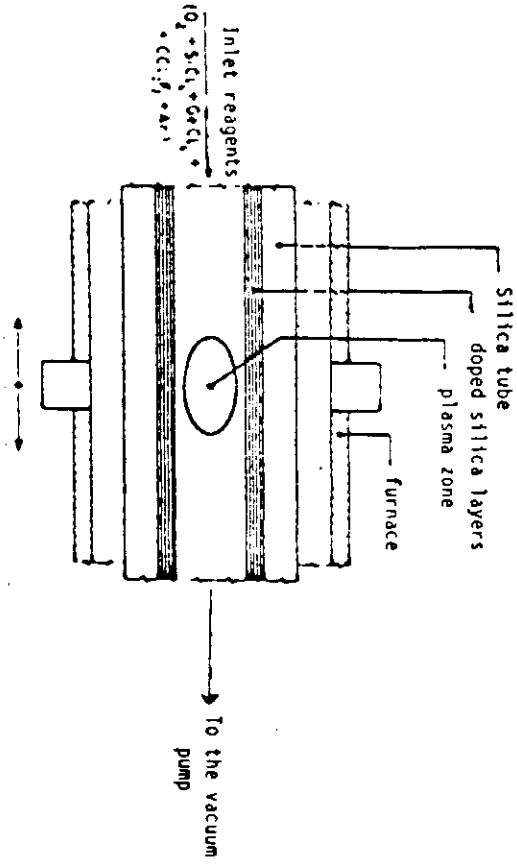


SCHEMATIC OF PCVD PROCESS

V A D PROCESS SCHEMATIC

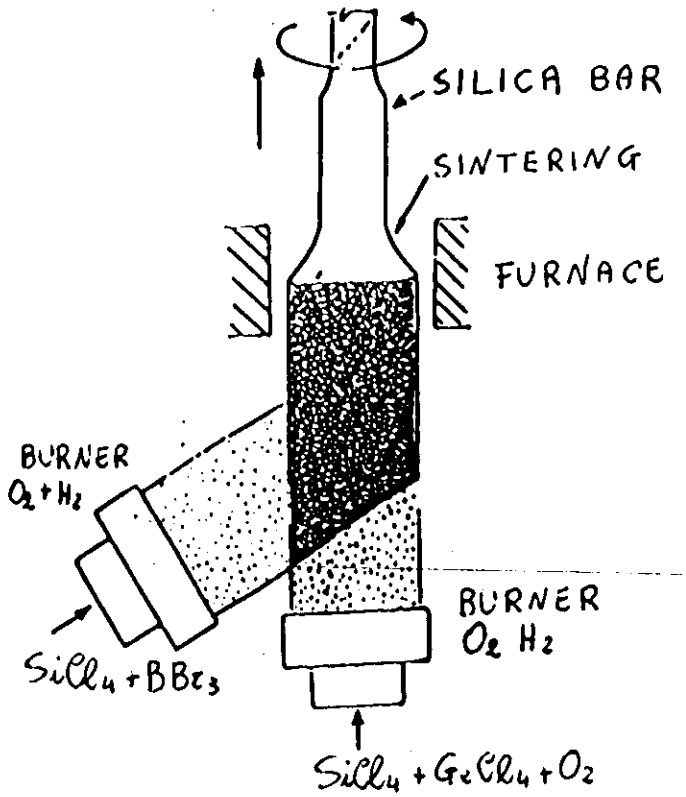


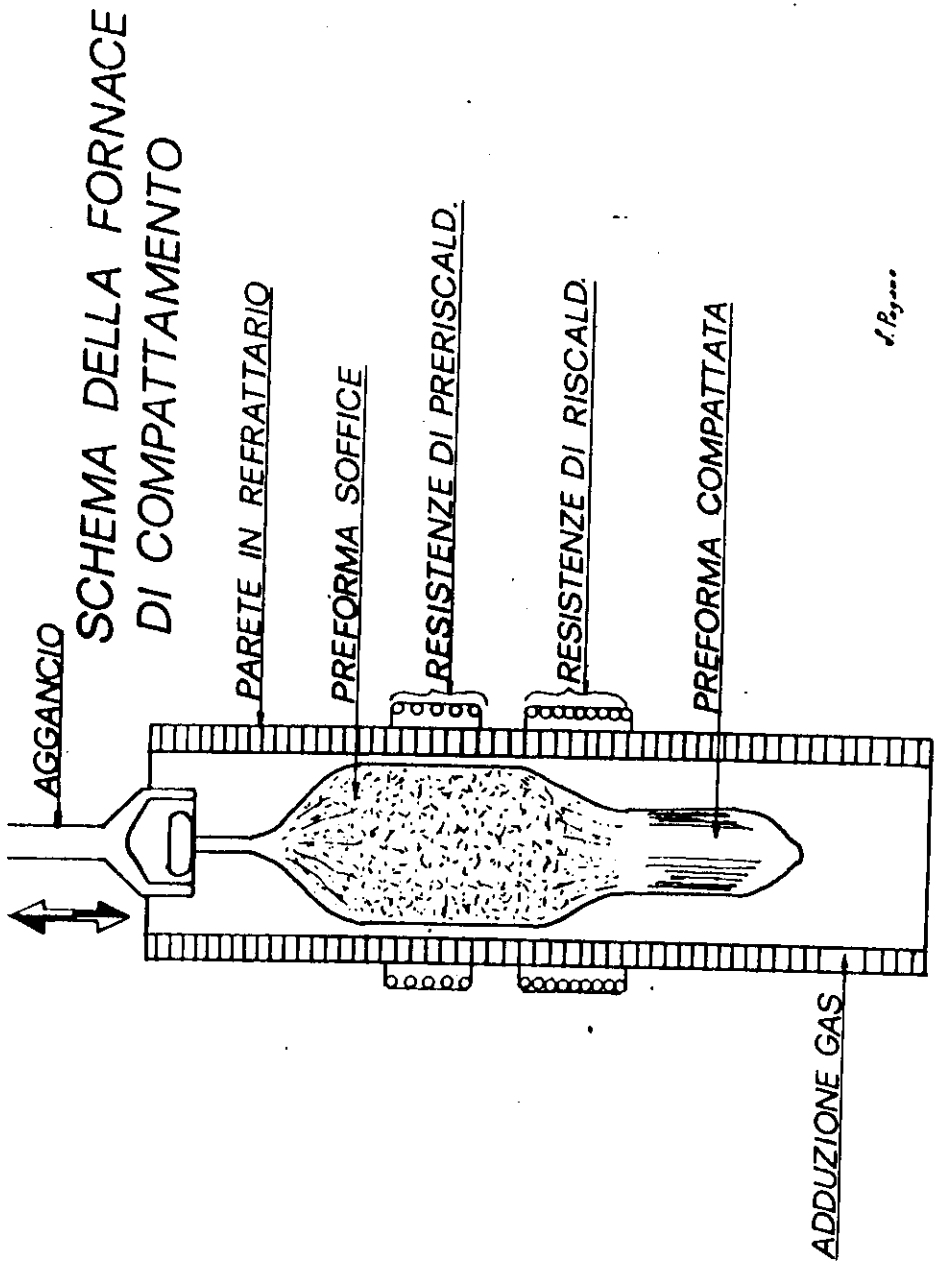

Fig. 10 - SCHEMA MACCHINA DI FILATURA

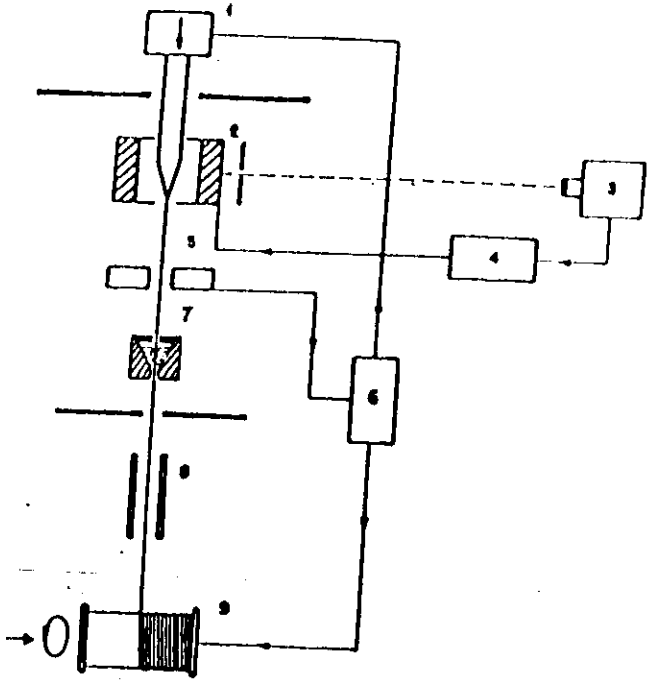


1) Apparato di alimentazione e PREFORMA
2) Fornace
3) Pirometro
4) Regolatore di temperatura
5) Misuratore di diametro
6) Regolatore della velocita' di filatura
7) Apparato per la prima ricopertura
8) Fornetto per l'essiccazione del polimero
9) Tamburo di tiro

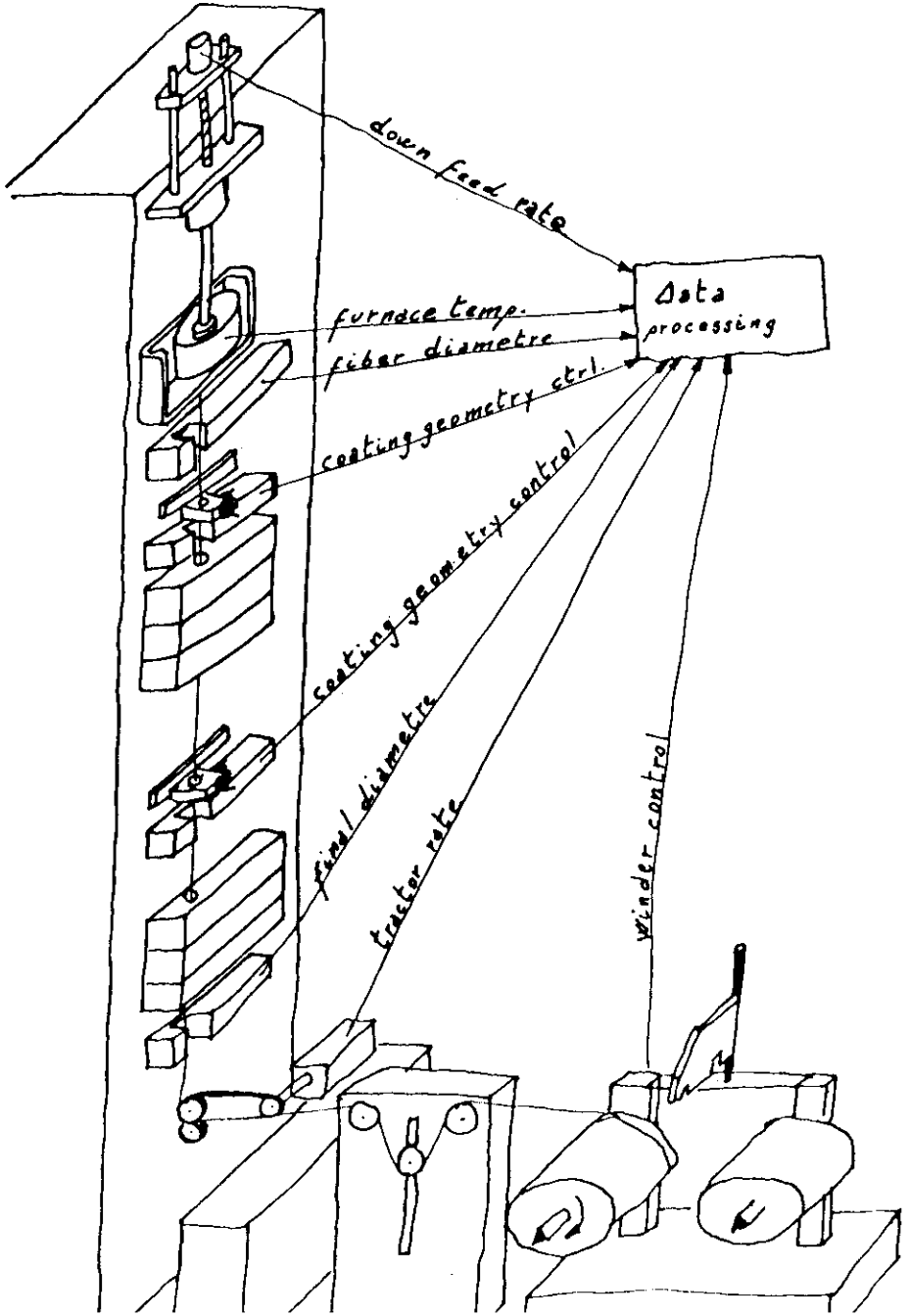

ATTENUATION 14-JAN-90 20:06:03 Len=25.700 km
FIBER ID:061090552504V
Categ/Tension:P L

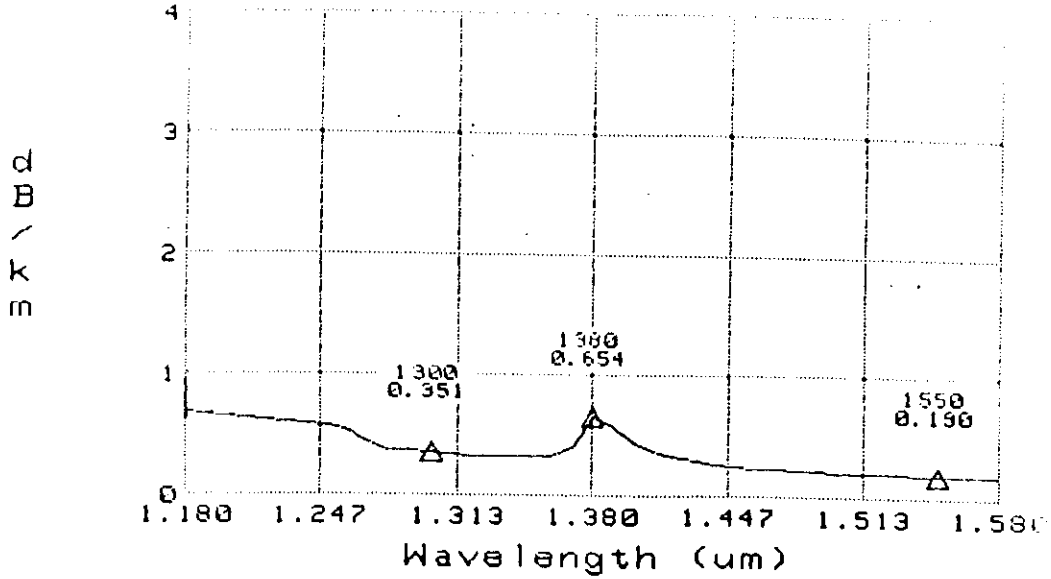


SPECATRESULT
Categ/Tension:P L
FIBER ID:061090552504V
Length=25.7000 km
Time of Test:14-JAN-90 20:06:03
Number of Entries:61

| (nm) | dB/km | (nm) | dB/km | (nm) | dB/km | (nm) | dB/km |
|---|---|---|---|---|---|---|---|
| 1000 | 0.954 | 1160 | 0.667 | 1320 | 0.328 | 1480 | 0.219 |
| 1010 | 0.920 | 1170 | 0.677 | 1330 | 0.324 | 1490 | 0.213 |
| 1020 | 0.884 | 1180 | 0.674 | 1340 | 0.324 | 1500 | 0.207 |
| 1030 | 0.851 | 1190 | 0.659 | 1350 | 0.326 | 1510 | 0.203 |
| 1040 | 0.818 | 1200 | 0.643 | 1360 | 0.330 | 1520 | 0.198 |
| 1050 | 0.787 | 1210 | 0.626 | 1370 | 0.398 | 1530 | 0.195 |
| 1060 | 0.758 | 1220 | 0.610 | 1380 | 0.654 | 1540 | 0.192 |
| 1070 | 0.731 | 1230 | 0.596 | 1390 | 0.590 | 1550 | 0.190 |
| 1080 | 0.705 | 1240 | 0.588 | 1400 | 0.453 | 1560 | 0.188 |
| 1090 | 0.683 | 1250 | 0.569 | 1410 | 0.373 | 1570 | 0.188 |
| 1100 | 0.663 | 1260 | 0.537 | 1420 | 0.320 | 1580 | 0.187 |
| 1110 | 0.647 | 1270 | 0.435 | 1430 | 0.287 | 1590 | 0.189 |
| 1120 | 0.634 | 1280 | 0.366 | 1440 | 0.265 | 1600 | 0.191 |
| 1130 | 0.632 | 1290 | 0.366 | 1450 | 0.249 | | |
| 1140 | 0.635 | 1300 | 0.351 | 1460 | 0.236 | | |
| 1150 | 0.645 | 1310 | 0.335 | 1470 | 0.227 | | |

# MISURA DELLA DISPERSIONE CROMATICA

FIBRA n. **shifted** LUNGHEZZA = **6410** mt DATA **18-02-1987**

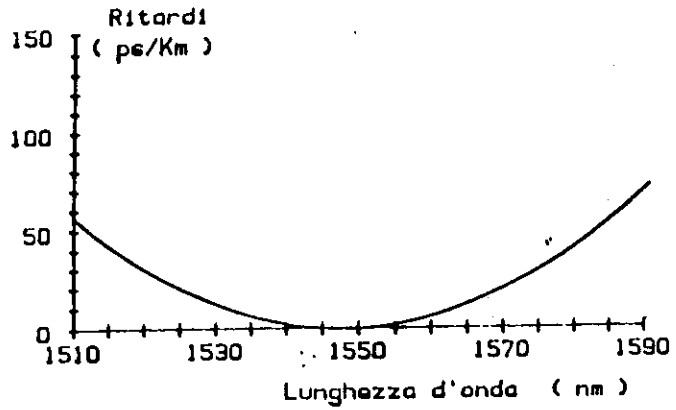


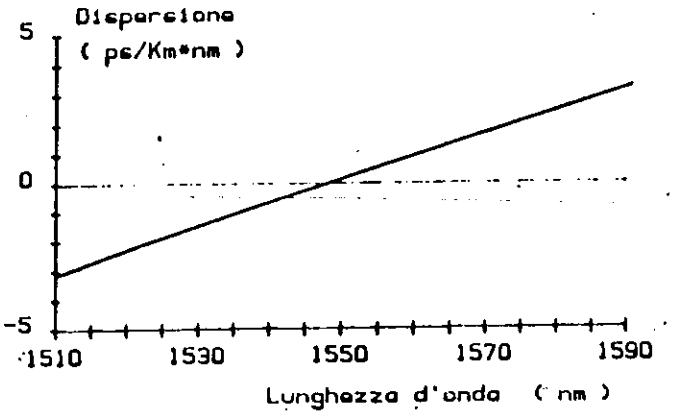


LUNGHEZZA D'ONDA A DISPERSIONE NULLA = 1547 nm

DISPERSIONE A 1550 nm = 0.25 ps/Km*nm

DISPERSIONE A 1530 nm = -1.37 ps/Km*nm

DISPERSIONE A 1570 nm = 1.79 ps/Km*nm

**F.O.S. S.p.a.**

Data : 14- 1- 1990

Fornace # : 1

Fibra numero : 041219552503 - TI

Lung. D'onda : 500 nm

| | | | |
|---|---|---|---|
| Diametro medio core | (um) | = | 8.8 |
| Diametro medio cladding | (um) | = | 125.8 |
| Errore di concentricita' | (um) | = | 0.28 |
| Errore di circol. del core | (%) | = | 2.39 |
| Errore di circol. del clad. | (%) | = | 0.54 |

Test code : 99

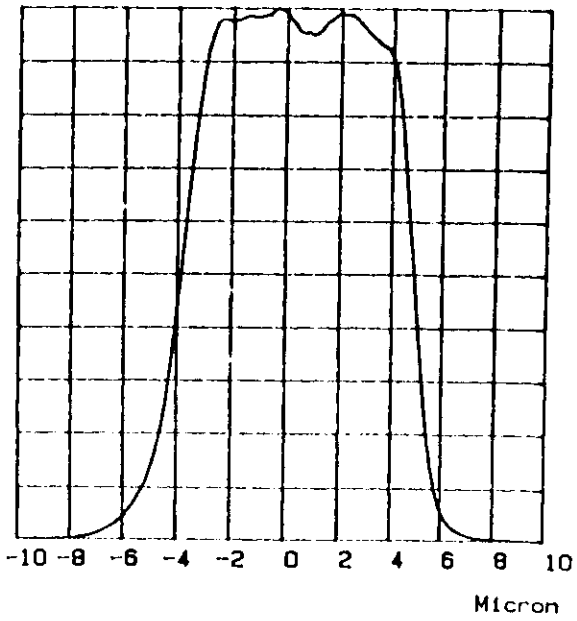


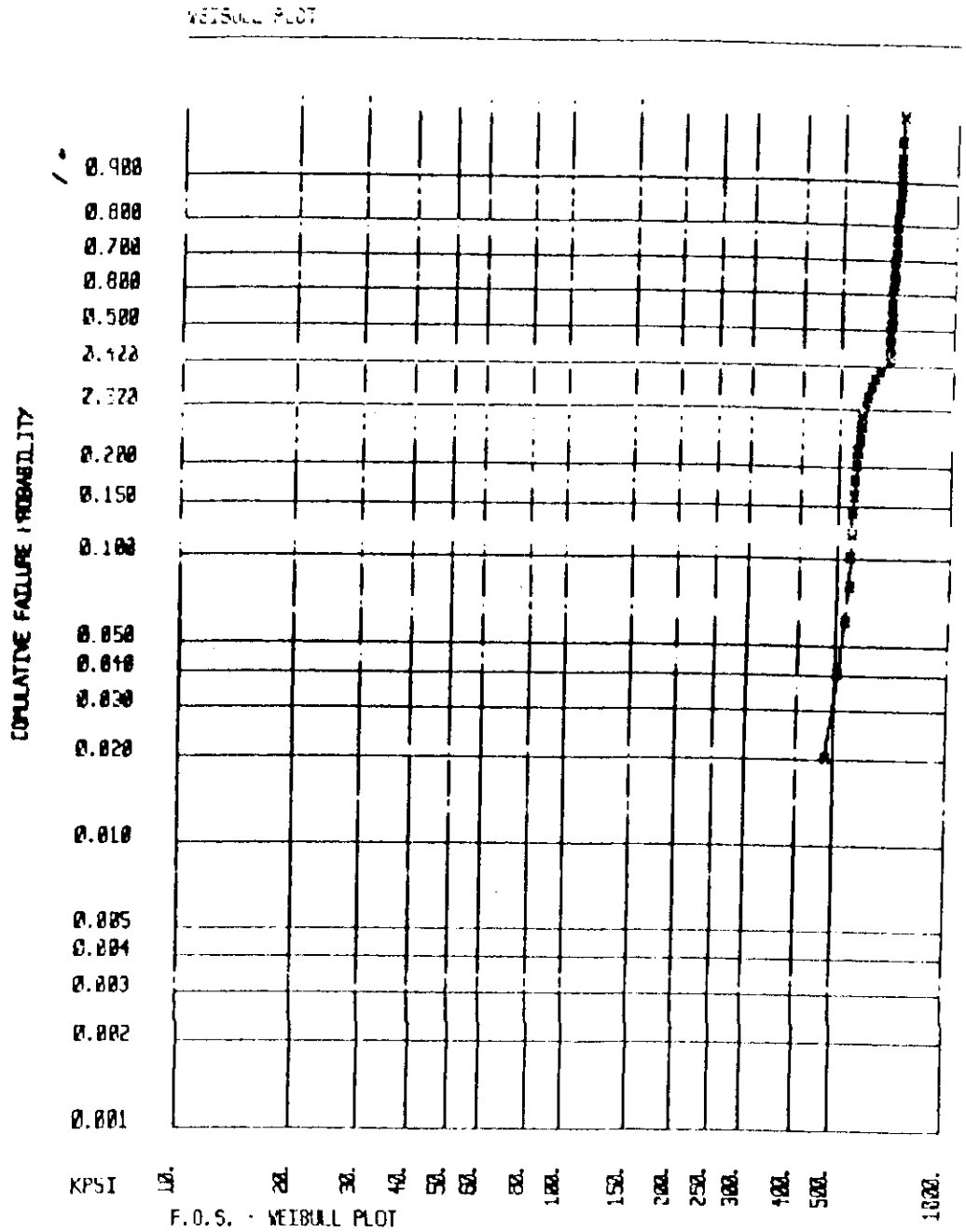

# FLUORIDE GLASS OPTICAL FIBRES IN TELECOMMUNICATION

G. COCITO - A. ZUCCALA*

CSELT Via G.Peiss Romoli, 274 TORINO ITALY

* F.O.S. Strada Prov.le 135-km.4,500 BATTIFAGLIA ITALY

## SUMMARY

Heavy metal fluoride glasses(HMFG) seem to be the most promising materials for optical fibres to be used in the telecommunication field. The minimum of their losses is in the spectral range of mid infrared at about $\lambda = 3$ μm. Here, a review is reported on the state of the art in the world.

## Introduction

Silica optical fibres, today normally used in the telecommunication field, are nearly perfect. They have attenuation very close to the theoretical minimum, and their chromatic dispersion may be reduced nearly to zero at the desired wavelength. They are able to cover distances of many tens of kilometers without repeaters. But if these distances are sufficient for the networks of several countries, mainly Europeans, they are not enough for transoceanic links hundreds of kilometers long. For this reason the most important telecommunication research laboratories in the world have started, some years ago, investigations on new materials with the aim of obtaining optical fibres having lower intrinsic attenuation. This characteristic, mainly depending on the Rayleigh Scattering, can be achieved with materials able to transmit in the MID Infrared Region (MIR). Several materials have been suggested for this aim : heavy metal oxides such as GeO2, chalcogenide glasses such as Ge-As-Se, cristalline halides such as AgBr and fluoride glasses such as BeF2 and Heavy Metals Fluoride Glasses (HMFG) ZrF4 based ( see figs.1 and 2).

This last category is considered the most promising one, because it has higher transparency related to oxide and chalcogenide glasses, superior glass forming ability with respect to chloride, bromide and iodide glasses and low degree of hygroscopicity and toxicity compared to BeF2 based glasses. The estimated theoretical attenuation of this material is around 1.E-02 dB/km close to 2.5 μm [1].

Until now the best reported result has been 0.7 dB/km on 30 m of multimode fibre [2]. To improve this value, the most critical problem is the elimination of the extrinsic losses due to the impurities inside the synthetized material as transition metals (Fe, Co, Ni, Cu), rare earths (Pr, Nd, Sm, etc....) and OH groups. Another important extrinsic attenuation loss must be searched in the defects induced during the construction of the fibre itself (bubbles, crystallization, geometrical irregularities etc...).

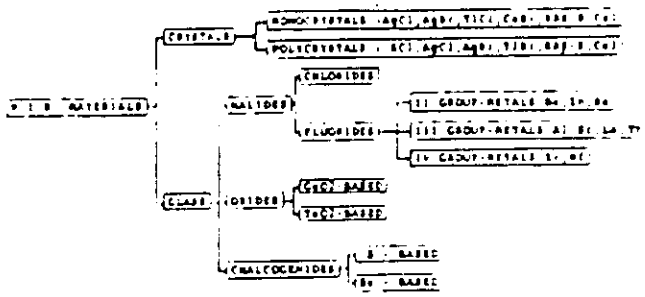


Figure 1 Classification of the materials used in the MID infrared

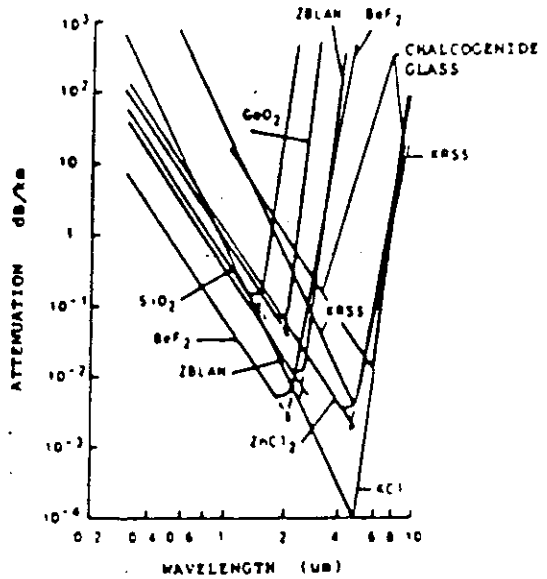


Figure 2 Attenuation intrinsic curves of the proposed materials for optical fibres working in the MID infrared.

Among the ZrF4 based glasses the most studied and promising composition is the so called ZBLAN that is ZrF4 -BaF2-LaF3-AlF3-NaF.

## Raw material purification and glass preparation

In the ZBLAN glasses, the zirconium fluoride ( ZrF4 ) and hafnium fluoride ( HfF4 ) are considered the mat

lakers (50-70% molar); other components as BaF2 are sed as matrix modifiers (20-30% molar) when the alcaine metals, transition metals and/or rare earths fluorides play the role of glass stabilizers.
he addition of AlF3, for instance, enlarge the working ange extending the vitrificability dominium.
he possibility of varying the refractive index of hese matrixes is given by the presence of the stabiliers compounds as PbF2 and BiF3 that increase it, or as iF, NaF, AlF3 that decrease it.
arying the quantities of the stabilizer, other imporant properties for the fibres can also be changed as: he thermal expansion coefficient, the tendency to crytallize, the transition temperature and the viscosity.
ome typical composition of fluorozirconate glasses are eported in Table n. 1 [3]. In this table also the glass ransition and the crystallization temperature are inicated. Δ = "Tx - Tg" is a parameter often used to valuate the stability of the glass : the higher Δ ,the igher the stability.
s a matter of fact to improve the glass stability, new ompositions are continuosly tested in the world labora ories. It's also important to mention that some glasses without ZrF4 or HfF4 have been proposed.
mong these, the most promising ones seem to be the lasses denominated BIZYT and composed by BaF2 - InF2 - nF2 - YbF3 - ThF4 [4]. These materials have an intrinic attenuation of 1 E-03 dB/km at 3.2 μm, and seem o be very attractive also in the active matrixes field lue to their easy dopability with metallic ions [5].
he synthesis of fluorozirconate glasses starts from he fluorides or from the respective oxides.
luorides are generally hygroscopic; therefore it's neessary to operate in an inert atmosphere (N2, Ar, He) r with reactant gases (such as SF6, CF4 etc..) that ave the capability to fluorurate the oxidic impurities nd to remove the water present. When starting from the xides the most common fluorinating agent is the Ammo ium bifluoride. The fluorination reaction takes place etween 300 °C and 400 °C and is followed by the meing - stage at 800 - 900 °C. The glass is obtained by apid quench from the liquid phase to the transition emperature and from this point, cooling down very lowly the glass to room temperature.
he allowable concentrations of transition metals and are earths in the fibre made with ZrF4 glass so that ome attenuation values lower than 1.E-2 dB/km could be eached, should be of the same order of μg/kg or lower 6 (see Table n.2).

| GLASS | ZrF4 | HfF4 | BaF2 | GdF3 | LaF3 | PbF2 | YF3 | AlF3 | NaF | LiF | Tg | Tx | Δ |
|---|---|---|---|---|---|---|---|---|---|---|---|---|---|
| ZBLA | 53 | - | 20 | - | 4 | - | - | 3 | 20 | - | 266 | 362 | 82 |
| ZBLALi | 49 | - | 25 | - | 3.5 | - | 2. | 2.5 | - | 10 | 256 | 349 | 93 |
| ZBLYAH | 47.5 | - | 23.5 | - | 2.5 | - | 2. | 4.5 | 20 | - | 261 | 335 | 74 |
| ZHBLYAH | 23.7 | 23.8 | 23.5 | - | 2.5 | - | 3 | 4.5 | 20 | - | 270 | 316 | 46 |
| ZBLALiPb | 51 | - | 14 | - | 5 | 5 | - | 3 | - | 20 | 275 | 357 | 82 |
| ZBLA | 53 | - | 20 | - | 5 | - | - | 4 | - | - | 320 | 392 | 72 |

Tab 1.
Matrix composition of based ZrF4 glasses.

is the impurities level of the commercial raw materials s usually higher than that, the key point to be faced s the research of methods to purify and analyse the tarting materials. Liquid phase methodologies seem o be the most interesting and effective; in particular "solvent extraction " ( 0.2 μg/gr of Fe in ZrOCl2, has been obtained ) [8] and ions exchange techniques (0.3n μg/gr of Fe in ZrOCl2) [9].
The Electromotive Series Displacement (ESD) has beer proposed; it is based on the reduction of the transition metals impurities with metallic zirconium added to a fused mixture of ZrF4 and BaF2. The difference between the reduction potentials of the impurities and of the zirconium is exploited (0.4 μg/gr of Fe in the mixture) [10].

| METAL | μg/kg a 2.5 μm | μg/kg a 3.5 μm |
|---|---|---|
| Fe | 0.04 | 1.1 |
| Co | 0.093 | 1.3 |
| Ni | 0.2 | 20.0 |
| Cu | 7.0 | - |
| Nd | 0.05 | - |
| Pr | 0.6 | 0.2 |
| Sm | 0.4 | 0.8 |
| Eu | 0.7 | 0.07 |
| Dy | 1.4 | 1.0 |
| Ce | - | 0.02 |
| Tb | - | 0.9 |

Tab. 2
Max. estimated concentrations of the impurities to obtain an attenuation of $10^{-3}$ dB/km at 2.5 and 3.5 μm

The "zone refining" technique [11] realizes the separation of the impurities from a monocrystal, concentrating them in a very narrow fused zone that flows away along the solid axis. The ZrF4 sublimation in an inert atmosphere [12] is still considered a basic method for the purification of this compound, also if it's difficult to reach levels lower than some μg/g.
Another proposed method is the synthesis of high pure ZrF4 based on the vapour phase deposition from a ZrBr4 -HF system [13]; and some researchers of GTE have experimented the " Chemical Vapour Purification " (CVP) based on the chlorination of metallic zirconium, followed by the treatment of the obtained chloride with a fluorinating agent [14]. The iron concentration in ZrF4 is resulted 0.140 μg/g. Lastly to eliminate the impurities of the oxidic types (OH, H2O, O= , etc..) many laboratories use the so called Reactive Atmosphere Processing (RAP) in which the glass preparation takes place in a reactive atmosphere of SF6, NF3, CF4 [15]. Also the analysis of the materials before and after, the purification represents a critical step of the process, since the use of very sophisticated techniques reaching the detection limits of μg/kg or less is necessary. At present, together with the atomic spectroscopy techniques ( absorption and emission), spark source mass spectroscopy and neutronic activation [16] are employed. For iron and rare earths determination ( in the finished glass ) photoluminescence techniques have been proposed [17].
Recently Griscom and coworkers have got ready an analysis method for the oxygen in the glass, based on ESR spectroscopy after a $\gamma$ rays bombardement of the sample. This method is able to detect 0.01 μg/g of O2 [18]. Combinated techniques as the atomic absorption with mass spectroscopy or ion-exchange chromatography will probably lower the detection limits.
The DSC, TMA and TG analysis are used to determine the characteristics of the glass i.e.: the glass trans. temperature (Tg), crystallization and melting temperature

(Tx and Tm), the thermal expansion coefficient and the possible losses or decompositions that the glass can undergo during the heat treatment.
The optical characterizations are mainly devoted to the glass transparence (IR, VIS, UV spectroscopy).
The structural studies are generally made with diffraction techniques (X rays and neutrons) and the results are often compared with computerized simulations (Molecular Dynamic Simulation - MDS).

## Manufacture techniques

One of the first techniques for making fluorozirconate glass fibres consists in the "built-in-casting" method [19].
In this case (see fig. 3) molten glass is poured in a cylindrical crucible. The portion of liquid that comes into contact with the mould, cools, increasing its viscosity. Therefore, overturning the crucible, it sticks to the walls, while the bulk of the glass flows out. In this way a plugged-bottom tube which is the clad of the preform, is obtained. After this step, the casting of the core is made, until the filling of the tube is achieved. Using this process, a high probability of bubbles and crystals formation at core-clad interface exists. The contamination of the glass from the environment is another possible disadvantage. These problems have been solved adopting the "Modified - built-in casting" method [20]. In this case the bottom of the crucible is removed after the casting of the clad, while this latter solidify to the walls. The depression due to the flowing out of the central part of the glass, simultaneously drags the molten core poured from the top. Another technique for making fluorozirconate glass preform is the "rotational casting" [21]. In a similar way to the "built-in-casting" method, molten cladding glass is poured into a preheated mould which is then swung into a horizontal position and spun at high speed. The glass cools slowly to form a tube and the core glass is then poured into this tube to make a preform. This assembly is then cooled and annealed.
All these techniques are really only suitable for step index multimode fibre, although variations have been proposed to obtain monomode dimensions by stretching and overcladding the preform. Also the "Jacketing method" and the "Suction method" [22] which are processes optimized and developed by the NTT, are used to make monomode fibres. In the former case the clad, separately prepared, is shrinked on the preform having the same diameter. In the "Suction method" the hole in the bulk of the glass is obtained by the contraction of the matrix during the phase of cooling and its dimension depends on a little setting-tank posed at the bottom of the crucible. In order to avoid the typical disadvantages of the processes based on the casting of liquid glass, new methods consisting in a vapour-phase deposition have been carried out. One of the most interesting among these ones is the RVT (Reactive Vapour Transport) method developed by Tran and coworkers in 1984 [23]. In this process the core is obtained by a vapour phase passing through a fluorozirconate glass tube that, owing to exchange and inclusion of Cl2, Br2, and I2, generates a layer at higher refractive index.
However, high difficulties exist in obtaining an efficient CVD method, due both to the slowness of the diffusion phenomena and to the low values of the vapour-pressures of these materials.

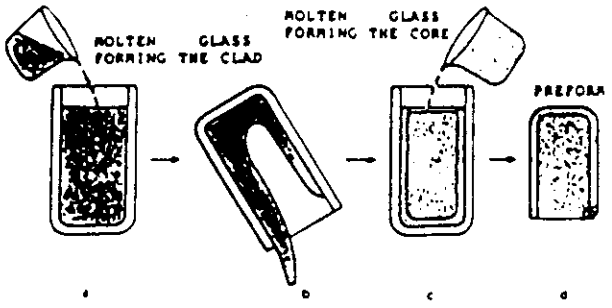


Figure 3
Operative scheme of the "built-in casting" method.
a) Casting of the molten glass forming the clad.
b) Emptying of the central part of the glass.
c) Casting of the molten glass forming the core.
d) Preform.

Poignant and coworkers have developed [24] a process to deposit thin glass-fluorurate layers by means of evaporation in vacuum-conditions.
The CVD is easily available only for the BeF2.
Miller and coworkers [25] have reported the following possible reaction in CVD conditions :
3 Be(CH3)2 + 2 BF3 = 3 BeF2 + 2 B(CH3)3
but we remind that, being BeF2 an extremely toxic and hygroscopic compound, its use should be avoided for commercial systems.
The preforms so obtained, are generally coated by teflon FEP and subsequentely drawn. In other cases "UV curable" polymers coat the fibre, immediately after the drawing of the fibre in a controlled atmosphere. The main difference existing between this step of the process and the correspondent one in silica fibre manufacture is the drawing temperature, varying in the range 200 °C - 400 °C. This parameter is very critical because the working range (Tx-Tg) is not particularly wide (about 100 °C in the stablest glass) and the formation of crystals strongly increases when T approaches the Tx value.
The drawing system must be always maintained in a N2 flow, in order to minimize the superficial crystallizations due to the moisture and to the atmospheric oxygen. An example of drawing tower is presented in fig.4.
Crucible techniques have been reported for direct drawing of molten fluorurate glass into fibre, but to date, reported losses have been very high. There are severe problems in using these crucible methods, originated by the poor glass stability and its succeptibility to thermal crystallization. However fluorurated fibres have been made by the double-crucible method.
Good results are obtained by the process reported in fig. 5 that is carried out in a completely controlled atmosphere and has a pressurization-system to pour the molten glass [26]. The most important variants of this method are the "single crucible" used by Drexage and coworkers [27] and the "triple crucible" [28] containing respectively core, clad and primary coating in a liquid phase. The former case uses a Pt-plugged-crucible where melting glass is obtained. This crucible has

a neck-shaped bottom maintained at a lower temperature with respect to the melting zone. This neck is followed by a water-cooled-Pt-cylinder. The fibre so obtained, is immediately coated by a plastic-layer in a crucible containing a polymeric material.
Finally the "Crucible preform drawing" worth to be mentioned. It allows to obtain the preforms contemporarely pouring the core and the clad by two concentric crucibles held into inert atmosphere [29].

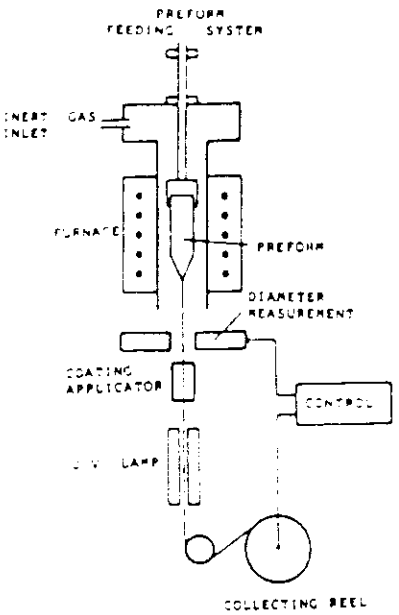


Figure 4
Scheme of a draw tower for fibres in fluorozirconate glass

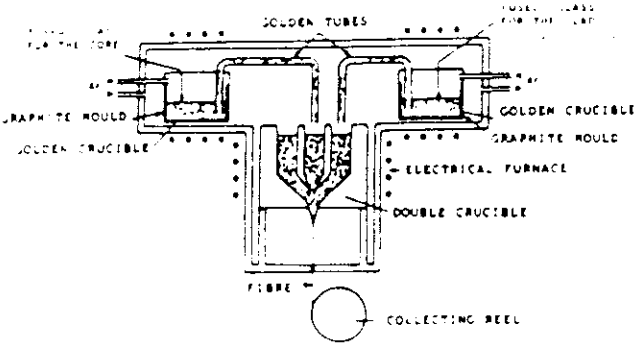


Figure 5
Scheme of the double crucible process developed at RADC

## Evolution of the research in the world

Presently, the most of the research in the U.S.A. is financied by the "Navy" and the "Air Force". Its fulcrum consists in some government-laboratories as the "Rome Air Development Center" (RADC) and the "Naval Research Laboratory" (NRL). These ones in turn financially support many others American centers. The RADC finances the studies about the chemical and physical properties of the heavy-halogenated glasses : for instance, the "Rensselaer Polytechnic Institute" has been entrusted with the research inherent to the viscosity, light-induced fusion, crystallization and glass-stability problems. Also the "Oklanoma University", with regard to the active fibres, and the "University of Florida", concerning the microstructures and the phase separation, is involved in the fluorozirconate glass project.
The NRL supports a more process-oriented research. As a matter of fact it financies the CVD application (for this particular kind of glasses) studied by CGw and the materials purification techniques studied by the "GTE laboratories". Today, in the U.S.A., the general interest seems addressed to the most immediately obtainable results in the field of the sensors, active fibres and other components.
In Japan the planning of the research about fluorurate glasses is very different. The biggest centers involved in this project operate in the telecommunication field (NTT, KDD, FURUKAWA) and the main objective seems to be the realization of fibres at very-low-attenuation. The study made in these laboratories is supported by the work about the characterization and the analysis of the glasses, effected by some universities (Tokio Institute of Technology, Kioto University).
In Europe the research is more dispersed and fractioned. Many telecommunication centers (BTRL, STL, CNET, CSELT, ect...), many universities (Rennes, Le Mans, Grenoble, Sheffield, Warwick, Clausthal, etc...)and many private industries (Le VerreFluoré, Schott Glaswerke, Siemens Ag, etc...), are engaged. The studies are oriented in : optical fibres realization, new glasses characterization, active fibres construction.
The best results obtained up to now (but only for short lenghts of fibre) are a 0.9 dB/km value of the attenuation at 2.6 μm obtained by NRL [30] and a 0.7 dB/km value at 2.2 μm from the researchers of the NTT [2].
On longer lengths (100m - 200m) BTRL has reported 3.9 dB/km at 2.6 μm.

## Fibres characterization

The determination of the optical and mechanical characteristics of this kind of fibres is the most investigated field. At 2.5 μm wavelength the main attenuation sources for fluorozirconate glass are assigned to : scattering wavelength independent, Mie's scattering and ionic absorption (Fe+2, Cu+2, Co+2, etc...). The first type of scattering comes from defects (bubbles, crystals, core clad interface flaws) larger than the transmitted wavelength. The "Mie scattering" varies in an inversely proportional way to the square of the wavelength and derives from defects of the same dimensions (1 μm) of the wavelength itself. With a value of these particles around 2000 per km, BTRL has extrapolated a "Mie Scattering" of 1.E-03 dB/km [31]. The spectral attenuation curve is normally obtained with cut-back methods using halogen lamp as a source, a grating monochromator and a Si or In-Sb photodetector. Specific absorption and "scattering" measurements have been performed using a Kr laser. The absorption is determined by a calorimetric method and the scattering through an integrating sphere and a Si photodiode [32]. As for the current silica fibres, also macrobending and microbending losses are evaluated [33].
The mechanical properties of the fibres are very impor-

tant for the telecommunication applications.
The main reason of the low tensile strength of these materials is the presence of surface defects to be especially ascribed to the crystalline-phases that can grow during the draw process. To avoid these phenomena some special drawing techniques have been tested. The intrinsic tensile strength of the fluorozirconate glass is estimated around 2 GPA (vs 10 GPA of silica fibre). Recently a value of 1.6 GPA has been obtained using bending strength measurements [34]. The feasibility of fusion-splicing for these fibres has also been claimed [35] and splicing losses of 0.1 dB/splice have been achieved.

## Considerations on the systems

The possibility of transmission in the MID-infrared on long repeaterless distances has also stimulated the research in the components field.
Thus semiconductor detectors $In_{1-x}$-$Ga_x$-As, In-AS-Sb and $In$-$As_{1-x-y}$-$Sb_x$-$P_y$ based, have been developed.
The most promising results is a Ga-In-As detector with a quantum-efficiency of > 90% out to 2.3 μm.
The development of semiconductor lasers working within the 2 - 3 μm range has been less rapid. Last year, the emission of an $In_{1-x}Ga_x$-As/In-As-P laser at 2.34 μm at low temperature was demostrated [36].
Several experimental systems based on multimode fluorozirconate fibres have been reported.
NTT has done a transmission experiment at 3.2 μm using a Pb-Cd-S diode laser as a 600 MHZ-modulated source and a semiconductor Josephson junction made of Ba-Pb-Bi-O cooled at liquid helium temperature, as receiver [37].
At BTRL a 34 MBIT/sec system has been realized, operating at room temperature at the wavelength of 2.5 μm [38]. It consists in a He/Ne laser externally modulated with a $Li$-$Nb$-$O_y$ waveguide modulator and a photodiode detector made from In-Ga-As/In-P with a receiver sensitivity of -35 dBm.
Some theoretical calculations have been done on the potentiality of a MID-IR system if all the components should be available. [31]
The results, considering certain assumptions for the system components, and with a fibre of 0.03 dB/km, show that is possible to reach a loss limited spans of 1500 km.

## Conclusions

Several laboratories in the world are hardly working in the field of fluorurate glasses for MID-IR transmissions. The results obtained up to now are encouraging. Current losses are one order of magnitude higher than that in the silica fibres, but on short lengths, very interesting values have already been obtained (0.7 - 0.9 dB/km). Values of 1.E-01 dB/km near the wavelength $\lambda$ = 2.5 μm, in some kilometers of fibres segments, are expected before 1992.
Chromatic dispersion will be better than 10 ps/nm.km between $\lambda$ =1.4 μm and $\lambda$ =2.6 μm. Also the development of the system components is progressing and some indications are that semiconductors lasers and detectors will soon be available at 2.5 μm.
In the fluorozirconate optical fibres technology, the purity at sub-ppb levels of the materials and the drawing process remain the most serious problems to overcome.
Therefore, it's a common feeling in the research community that, to reach the last hundredths dB/km, an entirely new process must be conceived.


## Acknowledgements

The authors gratefully thank the MIR group of CSELT (M. Braglia, M. Ferraris, G. Greco, E. Modone, G. Parisi) and V. Aulitto of F.O.S. for their helpful contribution.


## References


1. D.A. Pinnow, et al.,Appl.Phys.Lett.33,(1978),p.28
2. T. Kanamori, et al.,Jap.J.Appl.Phys.,6, 468, 198
3. O. Abollino, et al.,CSELT Int.Rep. N.RD88.426,198
4. A. Bouaggad, et al.,Mat.Rev.Bull.22, p. 685
5. P.S. Christensen, et al., 5th Int.Symp.Hal. Glas. (1988), p. 108
6. K.H. Sun, Glass Ind., 27 (1946), p. 522
7. A. Winter, J.Amer.Soc., 40,n.2,(1957), p. 54
8. G. Lu, et al., 4th Int.Symp.Hal.Glas.,Montery (1987), p. 21
9. P.H. Klein,et al., Opt.Eng.,24 (3), (1985),p. 517
10. M. Robinson, J.of Crystal Growth, 75,(1986).p.184
11. D.R. Gabbe, 3rd Int.Symp.on Halide Glasses, Rennes (1985)
12. M.G. Drexage, 3rd Int.Symp.on Halide Glasses, Rennes (1985)
13. K. Fujiura, et al.,Proc. 5th Int.Symp.on Halide Glas., Jap.,(1988), p.174
14. R.C. Folweiler, et al., 5th Int.Symp. on Halide Glas., Jap., (1988), p.533
15. Y. Noda,et al., 5th Int.Symp. on Halide Glasses, Jap., (1988), p. 162
16. R.C. Folweiler, et al., 4th Int.Symp.on Hal. Glas. Montery, (1987)
17. J.A. Freitas, et al.,Mat.Sci.Forum 19-20,1987 p229
18. D.L. Griscom,et al.,J.on non Cryst.Sol.103, 1988 p. 300
19. S. Mitachi,et al.,Elect.Lett.Vol.17,1981,p.591
20. J. Sakaguchi,et al.,J.Lightwave tech.,LT-5, N.9 1987, p. 1219
21. D.C.Tran,et al.,Elect.Lett.,18,659, 1982
22. Y. Ohishi,et al.,Elect.Lett.,Vol.22,1986, p.1034
23. D.C.Tran,et al.,Proc.OFC'84,New Orleans,1984, paper TUG. 2
24. H.Poignant, et al.,Glass Tech.,Vol.28,N.1,1987p.38
25. S.Miller;U.S.Patent n.4,378,987,April 1983
26. H.Tokiwa,et al.,El.Let.,V.21,n.24 1985,p.1131
27. M.Drexage,et al.,3rd Int.Conf.on I.O.-OFC 1981p.32
28. Y. Mimura,et al.,4th Int.Symp.on H.G.,M.CA,1987p69
29. T. Nakai, et al.Jap.Appl.Pb.,V.24,n.9,1986 p.L704
30. D.C. Tran, et al.,Proc.of SPIE,618,LA-Jan.86,p.48
31. P.W. France,et al.,Br.Tel.Tech.J.,V.5,N.2,1987p.29
32. M.V. Moore,et al.,Proc. 12th ECOC,Barcel.1986,p299
33. A.Mendez, et al.,Proc.of SPIE,V.843,S.Diego,1987
34. H. Schneider,et al.,Siemens Forsch.-u.Entwickl. Ber. Bd., 17, 1988, p.147
35. B.Harbison,et al.,F.O.C.'88,McLean,VA (Mar.1988)
36. R.U.Martinelli,et al.,OFC'88,NewOrleans,1988 TUC 6
37. Y.Enomoto,et al.,El.Let.,V.21,n.6,1985, p.219
38. R.A.Garnham,et al.,5th Int.Symp.on H.G.,Jap,1988